[redacted]

N67-26264
(ACCESSION NUMBER)
93
(PAGES)
CR-84013
(NASA CR OR TMX OR AD NUMBER)
(THRU)
1
(CODE)
11
(CATEGORY)
FACILITY FORM 602

NEWPORT BEACH OPERATIONS
PHILCO Ford
PHILCO-FORD CORPORATION
Space & Re-entry Systems Division
Newport Beach, California

1.

Publication No. UG-3934

SPACE AND RE-ENTRY SYSTEMS DIVISION

FINAL REPORT

for

IMPACT LIMITER DESIGN, FABRICATION AND TESTING

JPL CONTRACT NO. 951261

2 January 30, 1967

SUBMITTED TO: California Institute of Technology
Jet Propulsion Laboratory

PREPARED BY: Lunar and Planetary Programs
Space and Re-Entry Systems Division
3 Philco-Ford Corporation

APPROVED BY: _____

This work was performed for the Jet Propulsion Laboratory, California Institute of Technology, sponsored by the National Aeronautics and Space Administration under Contract NAS7-100.

TABLE OF CONTENTS

SECTION		PAGE
1	PROGRAM ACCOMPLISHMENTS	1- 1
2	TEST FACILITY	
	2.1 Air Gun Description	2- 3
	2.2 Gun Theoretical Velocity Expression	2- 8
	2.3 Instrumentation	2-10
	2.4 Test System Development Tests	2-13
3	BALSA SPHERE DESIGN AND FABRICATION	
	3.1 Limiter Design	3- 1
	3.2 Limiter Geometry	3- 5
	3.3 Segment Fabrication	3- 5
	3.4 Tetrahedron and Hemisphere Assembly	3-11
	3.5 Inner Payload	3-14
	3.6 External Cover	3-16
	3.7 Moisture Content	3-16
	3.8 Final Limiter Assembly	3-19
	3.9 Design Improvements in Sphere No. 4	3-19
4	BALSA SPHERE TEST PROGRAM	
	4.1 Test Report on Serial Nos. 1, 2, and 3 Balsa Spheres	4- 1
	4.2 Test Report on Serial No. 4 Balsa Sphere	4-16
	4.3 Weight Summary	4-23

SECTION 1

PROGRAM ACCOMPLISHMENTS

This impact limiter contract has brought about a significant increase in the knowledge of impact technology. The technology improvement was oriented toward large 45-inch diameter balsa spheres impacting at high speeds. Prior to the program the state-of-the-art had only progressed to 22 inch diameter spheres impacted at velocities up to 250 ft/sec. The major accomplishments which resulted from this program are:

(1) A test system was developed to successfully impact 300 lb 45-inch diameter spheres at velocities up to 426 ft/sec. The test system included: a unique air gun facility capable of propelling 1000-lb projectiles at speeds up to 500 ft/sec and developed trailing wire instrumentation which survives impact. This test system can be a substantial contributor in future impact technology efforts.

(2) The capability to fabricate balsa spheres was extrapolated in size from a 2-ft diameter to a 4-ft diameter. The tooling techniques utilized are also applicable to alternate materials and will allow even further extrapolation of size.

(3) Survival levels of payloads in balsa spheres were demonstrated at a velocity of 365 ft/sec with acceleration levels maintained under 4000 g.

SECTION 2

TEST FACILITY

The task required of the test system was to provide controlled impacts of large balsa test spheres (45 inch diameter, 300 lbs) at velocities up to 500 ft/sec providing impact acceleration data. In addition the impact area required surface interchanges ranging from rigid to powdered materials. In the investigation of facilities which would accomplish the requirements there was no known installation which could meet the criteria. Rocket sled test facilities were considered and(with special developments of payload separation from the sled)testing could be feasible for rigid surfaces. The horizontal facility possessed inherent difficulties with powdered non-cohesive surface targets (sand).

There were a few installations in the country that had developed successful pneumatic test systems for a 500 ft/sec velocity but they were primarily in the 6-inch diameter size range. These were in principal a blow gun with the test specimen acting as the piston and projectile. Facilities of this type generally suffered development pains in relation to high speed valving and instrumentation cabling. Once the facilities were developed and instrumentation problems solved pneumatic test facilities have proven to be highly reliable, and relatively low cost per test. The decision was made to tackle the problem with a unique facility with a substantial scale-up of existing state-of-the-art.

The configuration necessary for a variation of impact target materials is a vertical gun shooting down into a target material pit. The test facility schematic in Figure 2-1 shows the basic elements of the test facility. The target material pit is a 10 ft deep 15 ft X 15 ft concrete lined cavity which contains the seismic block impact surface. The pit wall provides the foundation for the gun and handles the quarter of a million pounds of

FIGURE 2-1
TEST SETUP

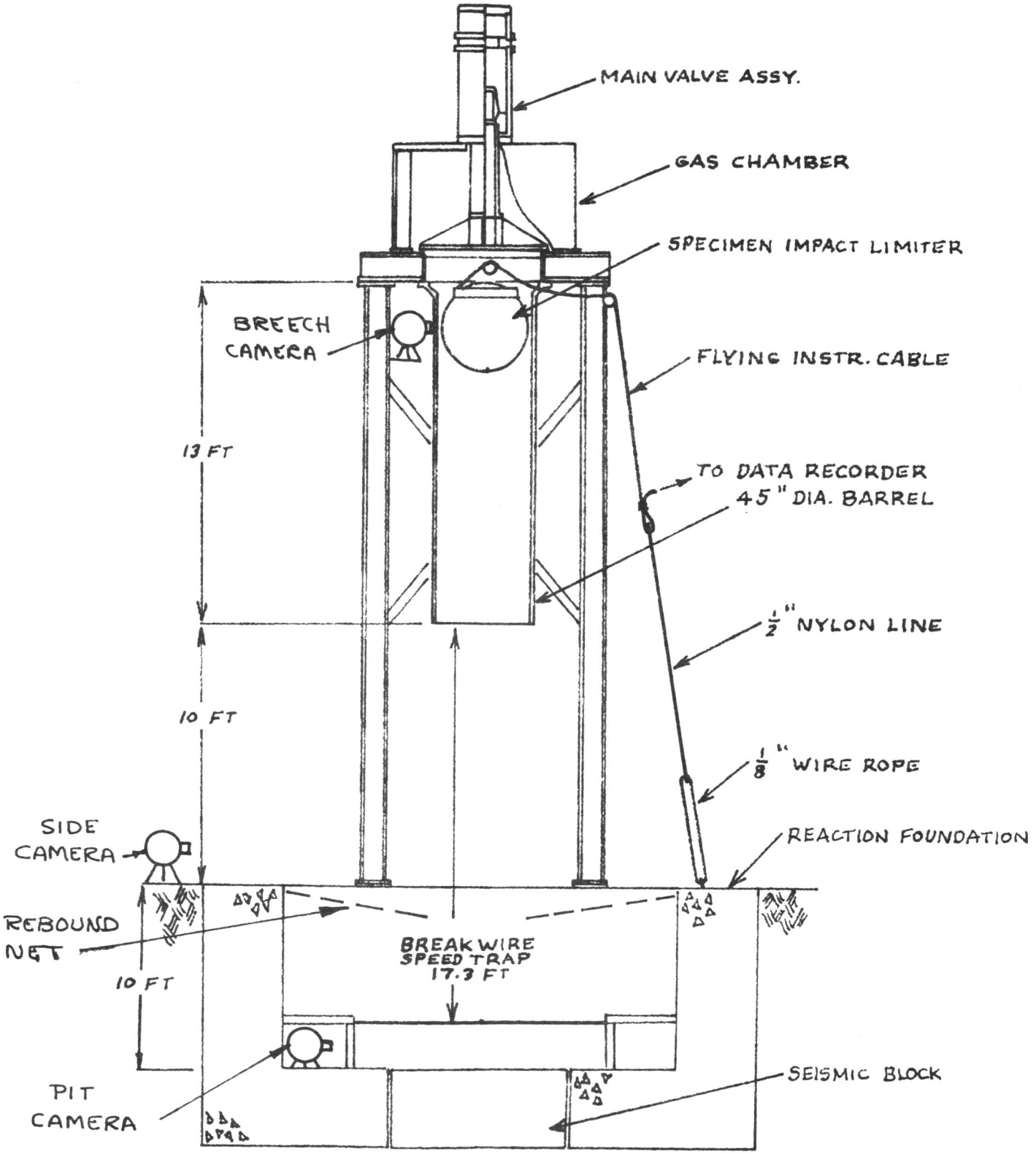

gun reaction loads. With the rebound net (Figure 2-2) and the deep pit walls, protection is provided against high speed impact debris. Also located in the impact pit are a fastex camera and speed trap break wire (Figure 2-3). The air gun is mounted directly above the impact area on a crosshead located 23 ft above the ground supported by "H" beam legs. The gas chamber and valving is located above the crosshead while the gun barrel and specimen are located below (Figure 2-4). A photo of the gun (Figure 2-5) during the actual firing reveals the cloud which obscures the barrel. This cloud propagates directly behind the projectile and hampers high speed photographic studies of impact. It is caused by the expanded low temperature nitrogen condensing moisture in the atmosphere. The nitrogen banks which charge the gas chamber are shown in the foreground.

2.1 AIR GUN DESCRIPTION

The Air Gun is basically a velocity generator designed to accept a relatively large test item and to accelerate the item to a terminal velocity of 500 ft/sec. The payload acts as a piston in a long cylindrical barrel with air pressure providing acceleration forces through the barrel length. A 325,000 in^3 tank stores compressed nitrogen at up to 135 psi provides the energy source. It is necessary to employ a relatively large flow area valve system to release the gas volume in adequate quantity to maintain a high gas pressure on the test projectile. The inlet passageway is 54.0 in. in diameter. The effective acceleration stroke is 132 in. with a 45.63 in. diameter barrel.

The gas is contained within the chamber by a large flat seat valve seating directly across the orifice. The lower surface of the seal head contains a circular rubber seal ring which makes contact with the top surface of the orifice tube flange. A tubular steel shaft is attached to the top of the seal head and extends through the gas chamber and into the main valve cylinder. The valve open piston is located on this shaft. It provides the force to raise the seal head 18.0 in. in approximately .012 sec. The two side valves provide high pressure gas to activate the valve open piston. When the seal head is opened it is accelerated rapidly upward and must be stopped. A deceleration metering pin is attached to the top of the main valve piston within a water reservoir. After an upward travel of approximately 18.0 in. the metering pin enters an orifice causing a water metering process to occur to decelerate the main valve.

The side valve which activates the sequence contains the high pressure gas chamber and a quick opening valve. The quick opening valve which operates in .001 sec is contained by a hydraulic lock. The hydraulic lock is vented by a solenoid valve thereby releasing the valve piston.

This valve system provides two major features: the firing event is operated remotely within milliseconds allowing coordination with instrumentation and photography. The main valve operates fast enough to reduce gas inlet loses and provides efficient energy transfer to obtain high sphere velocities.

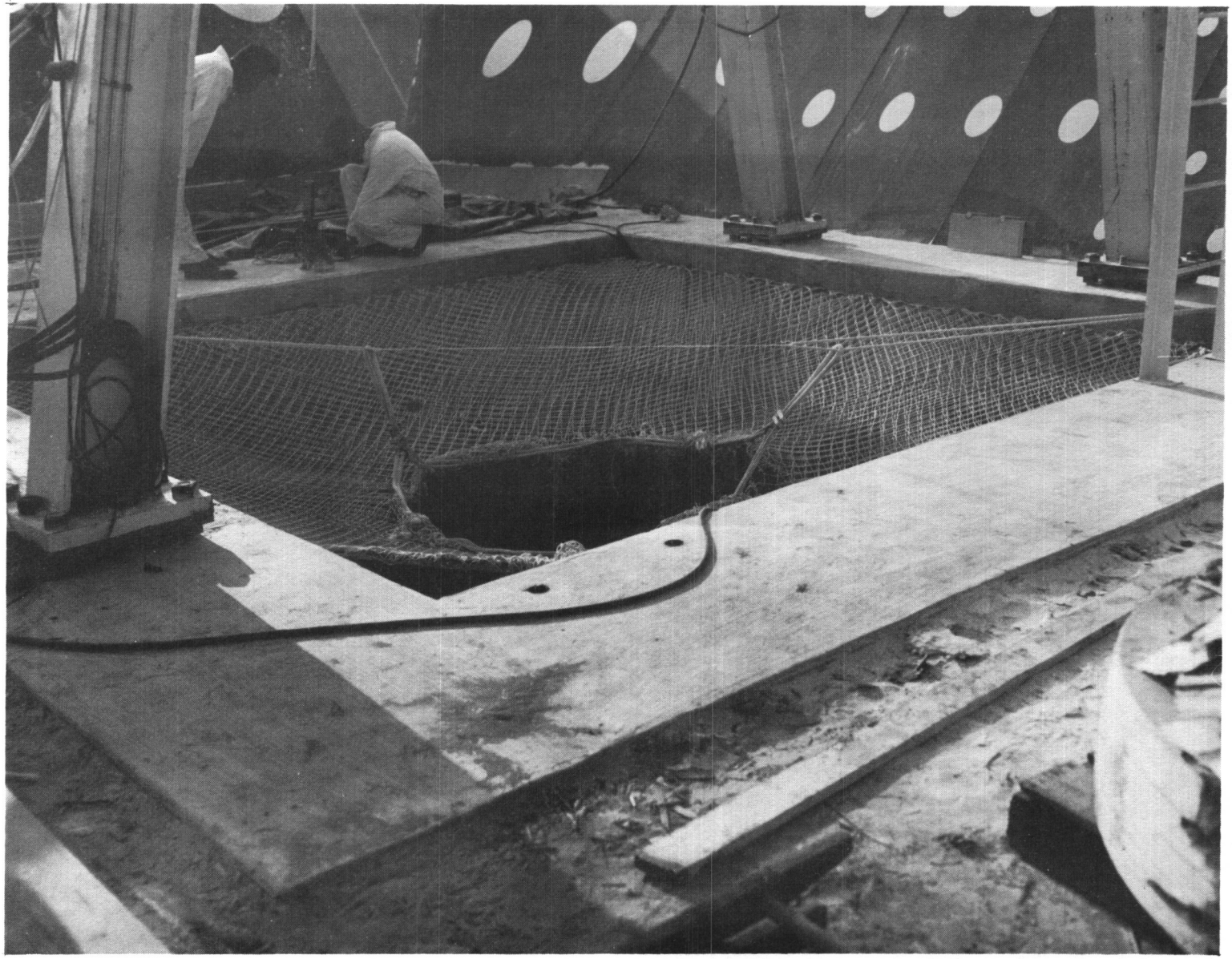

FIGURE 2-2 REBOUND NET

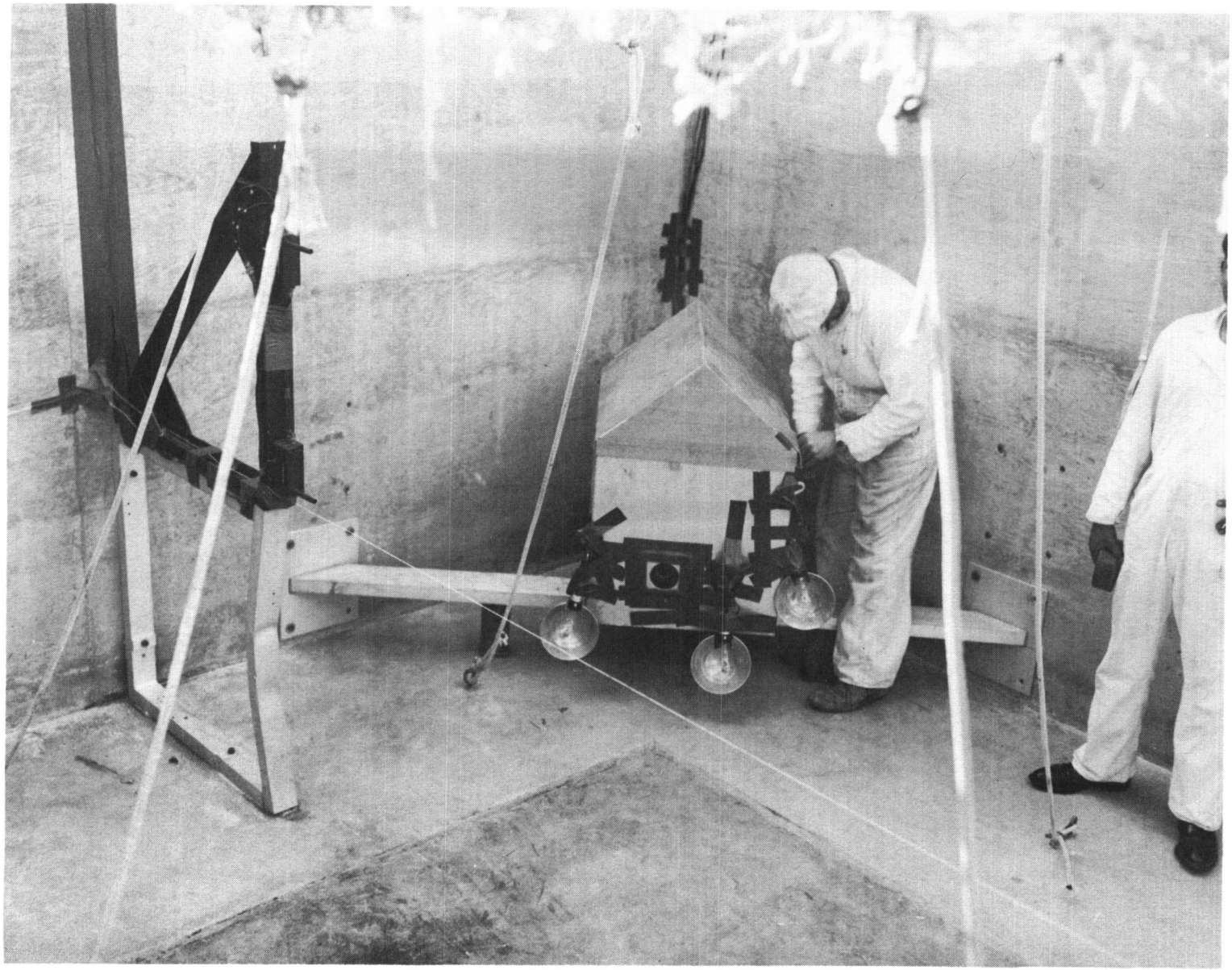

FIGURE 2-3 IMPACT PIT

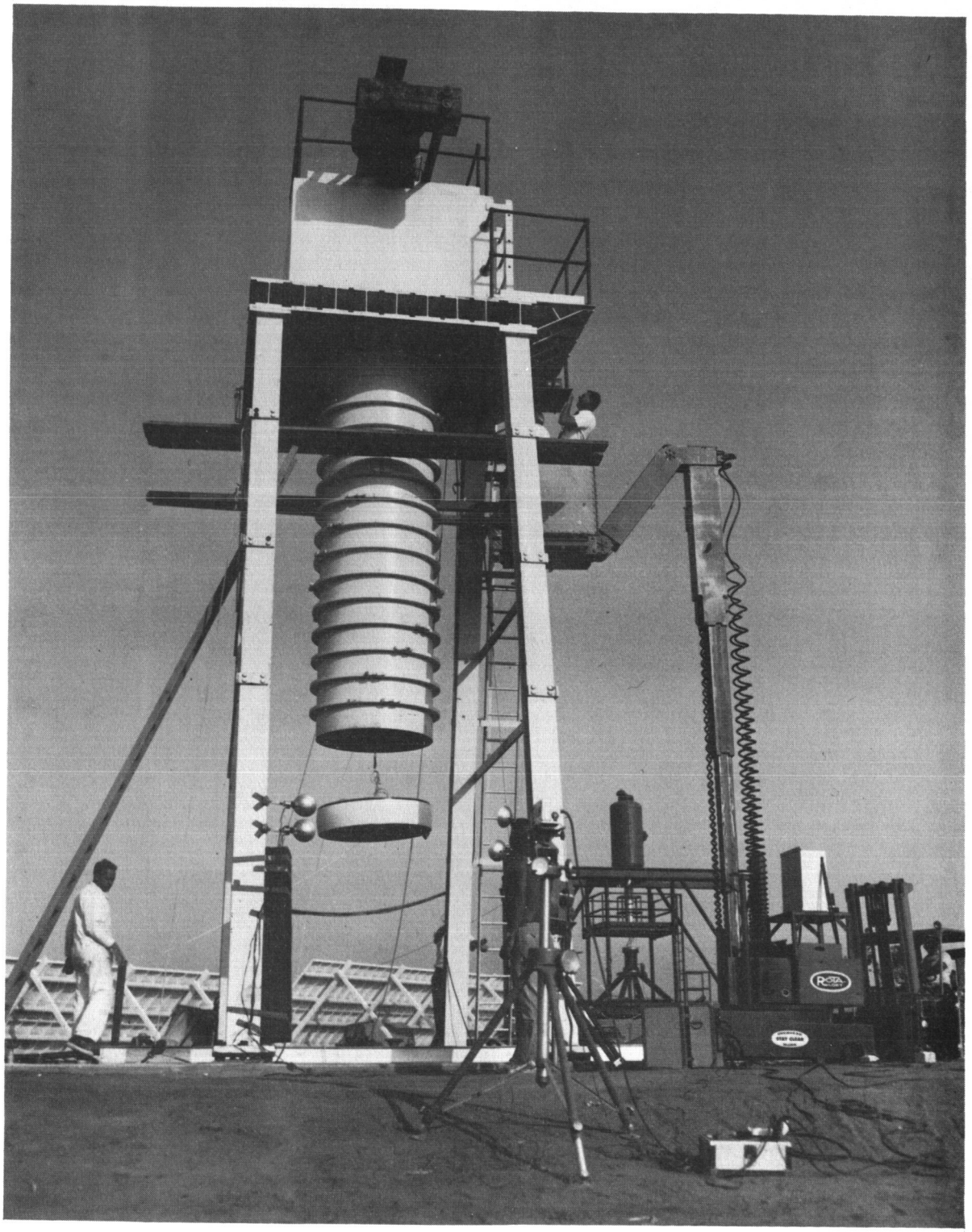

FIGURE 2-4 AIR GUN

FIGURE 2-5 AIR GUN FIRING

A motor-winch assembly provides the means of lifting the test sphere into the breech. It is attached to one side of the cross head. A shaft extends across the orifice tube containing a pulley which directs the lifting cable down at the center of the barrel. The sphere is maintained in position by a short cable fuse link which breaks at approximately 500 lbs force provided by the inlet gas pressure.

2.2 GUN THEORETICAL VELOCITY EXPRESSION

A relationship of projectile velocity with the gun set pressure and projectile weight is essential to predicting performance with minimum trial and error. The fundamental equation denotes an energy balance with the work done by the expanding gas equal to the kinetic energy of the test projectile. The work done by the gas is a direct function of the pressure directed upon the payload and the stroke. The pressure is operated on by a breech volume void and further by pay load movement. These pressure drops can be accounted for by the gas laws for isentropic expansion of gas. The fundamental energy equation follows:

WORK BY EXPANDING GAS - WORK AGAINST ATMOSPHERIC PRESSURE = PROJECTILE KINETIC ENERGY

$$\int P\ (s)\ A\ ds - P_A\ A = \frac{1}{2}\ \frac{W}{g}\ V^2 \qquad (1)$$

Where:

P(s) = Function of pressure relation to payload movement

A = Barrel area - 1590 in^2

S = Payload displacement - 132 in

P_A = Atmospheric Pressure - 14.7 psi

W = Payload Weight - lbs

g = Acceleration of gravity - 32.2 ft/sec

V = Payload velocity - ft/sec

The pressure relationship of the breech pressure with stroke is established by the isentropic expansion of gas.

$$P\ (s) = P_o \left[\frac{V_o}{V_s} \right]^{1.4}$$

$$\therefore P(s) = P_o \left[\frac{V_o}{V_o + A \cdot S} \right]^{1.4} \qquad (2)$$

Where:

P_o = Pressure of gas above payload before payload moves.

V_o = Volume of air in tank plus breech void
= 325,000 in^3 + 35,000 in^3
= 360,000 in^3

V_s = Total volume at any stroke

The relationship of the tank set pressure is also established by the isentropic expansion of gas.

$$P_o = P_{set} \left(\frac{V_{tank}}{V_o} \right)^{1.4}$$

$$P_o = \left(\frac{325,000}{360,000} \right)^{1.4} P_{set}$$

$$P_o = .870\ P_{set} \qquad (3)$$

Substituting (3) into (2)

$$P(s) = .870\ P_{set} \left[\frac{V_o}{V_o + A_s} \right]^{1.4} \qquad (4)$$

Substituting (4) into (1)

$$\left[.870\ P_{set}\ A\ V_o^{1.4} \int_o^s \left(\frac{1}{V_o + A_s} \right)^{1.4} ds \right] - \left[P_a\ A \right] = \frac{1}{2} \frac{W}{g} V^2 \qquad (5)$$

Integration and substitution of constants results in the following expression:

$$V = 232 \sqrt{\frac{.130\ P_s - 3.08}{W \times 10^{-2}}} \qquad (6)$$

Where:

V = Projectile velocity - ft/sec

P_S = Absolute set pressure- psia

W = Projectile weight - lbs

This equation is presented in Figure 2-6 with a plot of gun gage pressure versus velocity with three different payload weights. Actual test data is plotted on this curve showing excellent correlation. The test points are all within 5 percent of the theoretical curve.

2.3 INSTRUMENTATION

An accelerometer and breakwire speed trap were used to measure impact deceleration and speed respectively. High speed motion picture coverage was supplied to give photographic data.

The accelerometer instrument package consisted of a cylindrical steel plate to which were mounted a mechanical termination for the signal cable and an Endevco Model 2261M6 accelerometer. The instrument package was mounted into an aluminum ballast plate within the maple payload via a 3-in. diameter access hole provided through the upper limiter half. USS Amergraph Type 4-H-219-B electro-mechanical cable was used to supply power and carry signals from the accelerometer. The cable is armored with double reverse layers of performed high strength steel wire and has a rated breaking strength of over 4000 lbs. The cable was routed from the instrument package to the top of the sphere, then to the bottom of a sheet aluminum ring which was bonded to the surface of the sphere at about latitude 45^{o}. Seven turns of the cable were layed on the coil form in a clockwise sense and lightly bonded to it. Twenty feet of cable were left free for connection to the test facility instrumentation system (Figure 2-7).

As the limiter travels downward, the instrumentation cable pays out from its coiled position on the limiter. Tensile loads in the instrumentation cable are reacted outside of the blowgun system via guide and pulley systems. A 10 ft length of 1/2-inch nylon line is used as a buffer to smooth transient shock loads which could otherwise result in cable failure at the rigid anchor point.

Impact speed was determined from the time interval required for the specimen to break two wires spaced 17.3 ft apart. One breakwire was tied across the blowgun muzzle and the other was located about 3 ft above the impact target. As each wire was broken, an electrical circuit was interrupted. The breakwire events and accelerometer data were recorded on an oscillograph with a time base of 10 milliseconds/in. using CEC7-326 galvanometers which have a flat frequency range from 0-3000 H_z and linear phase response.

FIGURE 2-6

PROJECTILE VELOCITY

$$V = 232 \sqrt{\frac{.130\, P_s - 3.08}{W \times 10^{-2}}}$$

P_s = SET PRESSURE PSIA

W = PROJECTILE WT. LBS

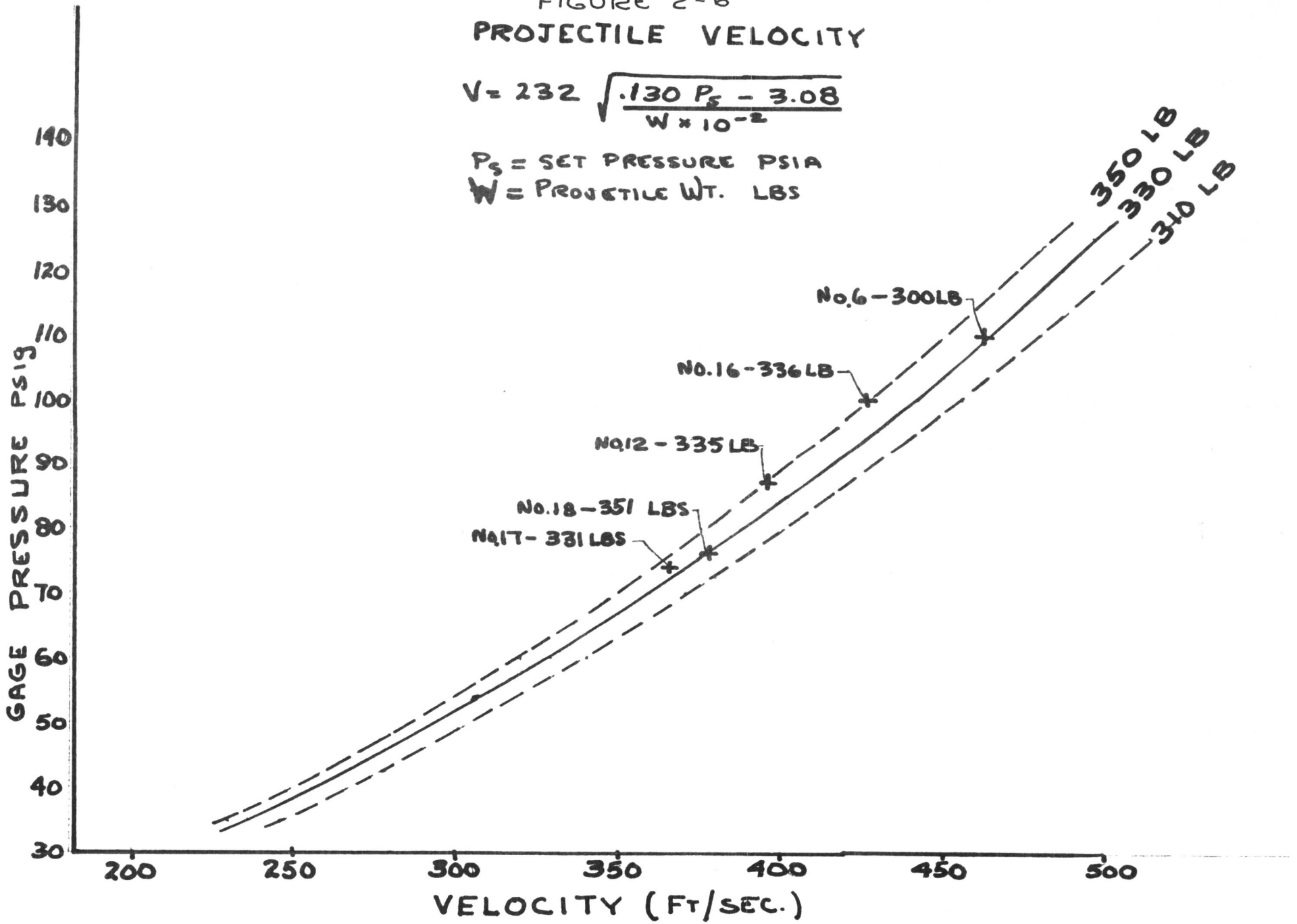

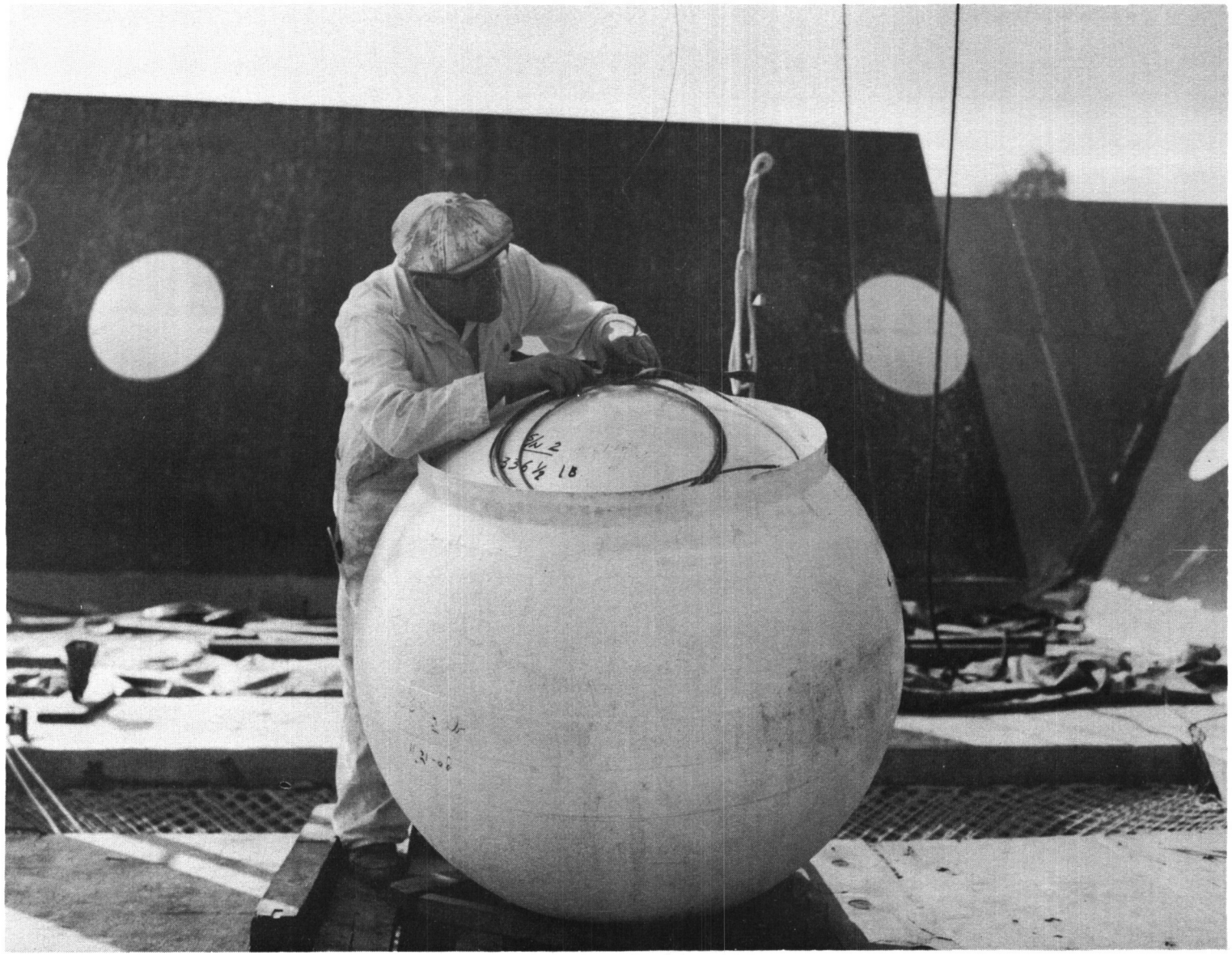

FIGURE 2-7 TEST CABLE INSTALLATION

High-speed motion picture cameras were placed (1) at the gun breech to record cable dynamics, (2) at the ground level to record the action of the limiter as it leaves the blow gun muzzle, and (3) at the target level to record the impact dynamics.

2.4 TEST SYSTEM DEVELOPMENT TESTS

The test system experienced considerable development pains. The problems were concentrated in two primary areas; the air gun valve and the instrumentation cable.

The evolution of the solution of the problems were through test firing of dummy projectiles. There were 15 dummy shots made prior to obtaining a complete test system. This required considerable expenditure of time and money to create projectiles, conduct tests, tear down and repair the gun, diagnose problems and design solution. There were three kinds of test projectiles utilized; plywood disks, plywood spheres and fiberglass spheres. (Figures 2-8, 2-9, and 2-10). The plywood dummies were quite representative while the fiberglass units were structurally unsound failing at launch.

The air gun experienced four problems of a major nature each of which required complete teardown of the machine at different times along the program. The initial problem was that the high pressure air reservoir was too small to open the valve at high velocity shots. This was corrected by adding an additional tank on the side valve. This corrected that problem but caused a new one; with the added tank the side valve support attachment was inadequate and had to be beefed up. Continual problems were had with the side valve housing seal due to pinching at assembly. A redesign corrected the problem. The main valve piston seal also required intermittant replacement. Due to the massive size of the equipment even seal replacements were a major operation requiring cranes and heavy handling equipment.

Superimposed on the air gun problems was a program to establish a trailing wire configuration which would survive at 500 ft/sec . A great many wire systems were attempted prior to the successful system developed. The fundamental elements in the instrument wire system were the instrument wire, the tether, the cable restrainer and the cable playout. The physical deterrants to success were air blast, projectile acceleration, cable shipping, gun barrel abrasion, and wire inertial. In all cases the cable was stowed and played out from the projectile. Each of the systems tried succumbed to one or the combination of the forces in the system.

The final solution contained elements which counteracted the previous pitfalls. The basic wire was a four wire conductor mounted in the center of a two-layered steel cable shroud. The steel cable protected against abrasion loads. It was stowed in a cylindrical configuration bonded to an aluminum holding ring. This accomplished two things, the cable stayed on

FIGURE 2-8 45-INCH PLYWOOD DISC PROJECTILE

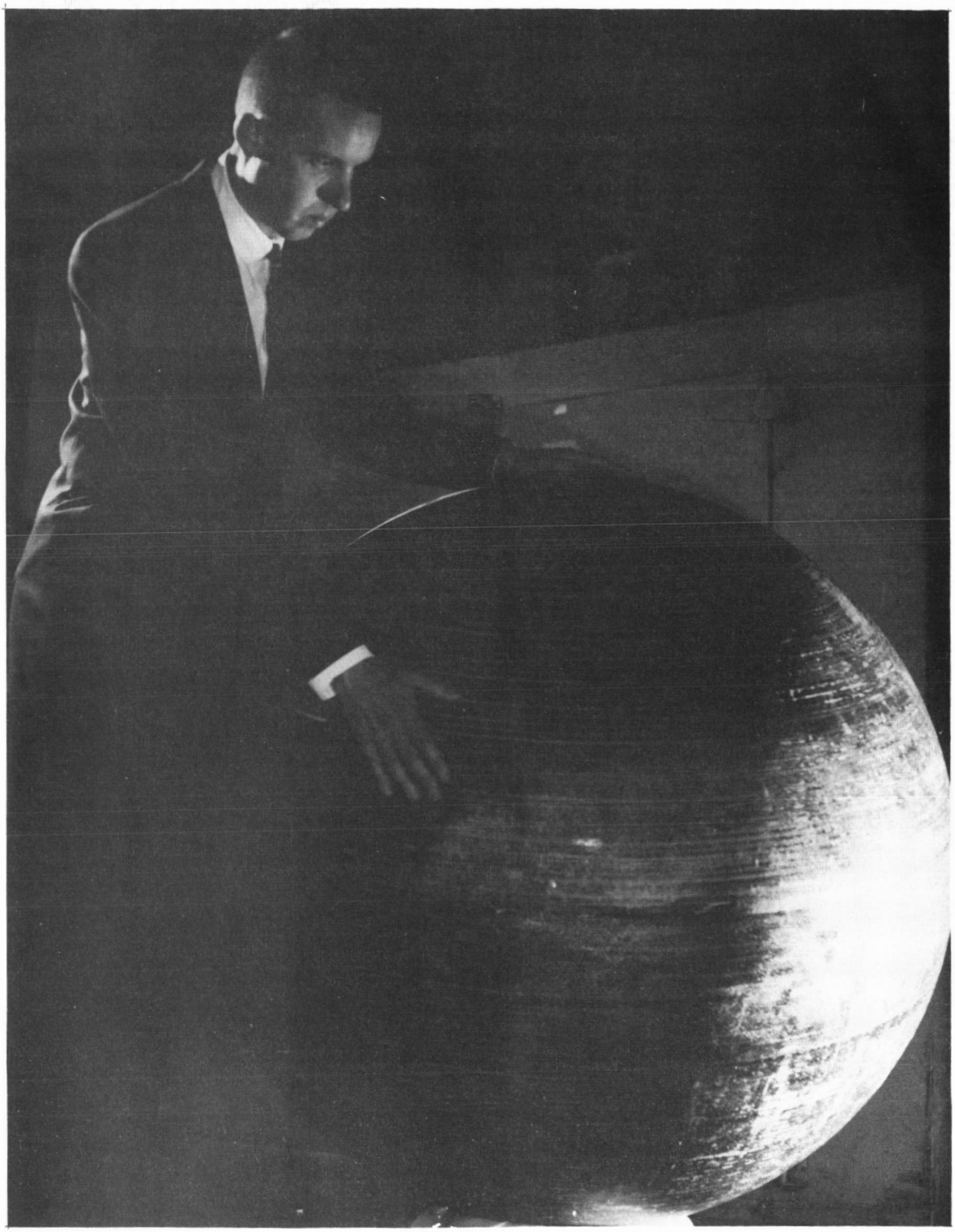

FIGURE 2-9 45-INCH PLYWOOD SPHERE PROJECTILE

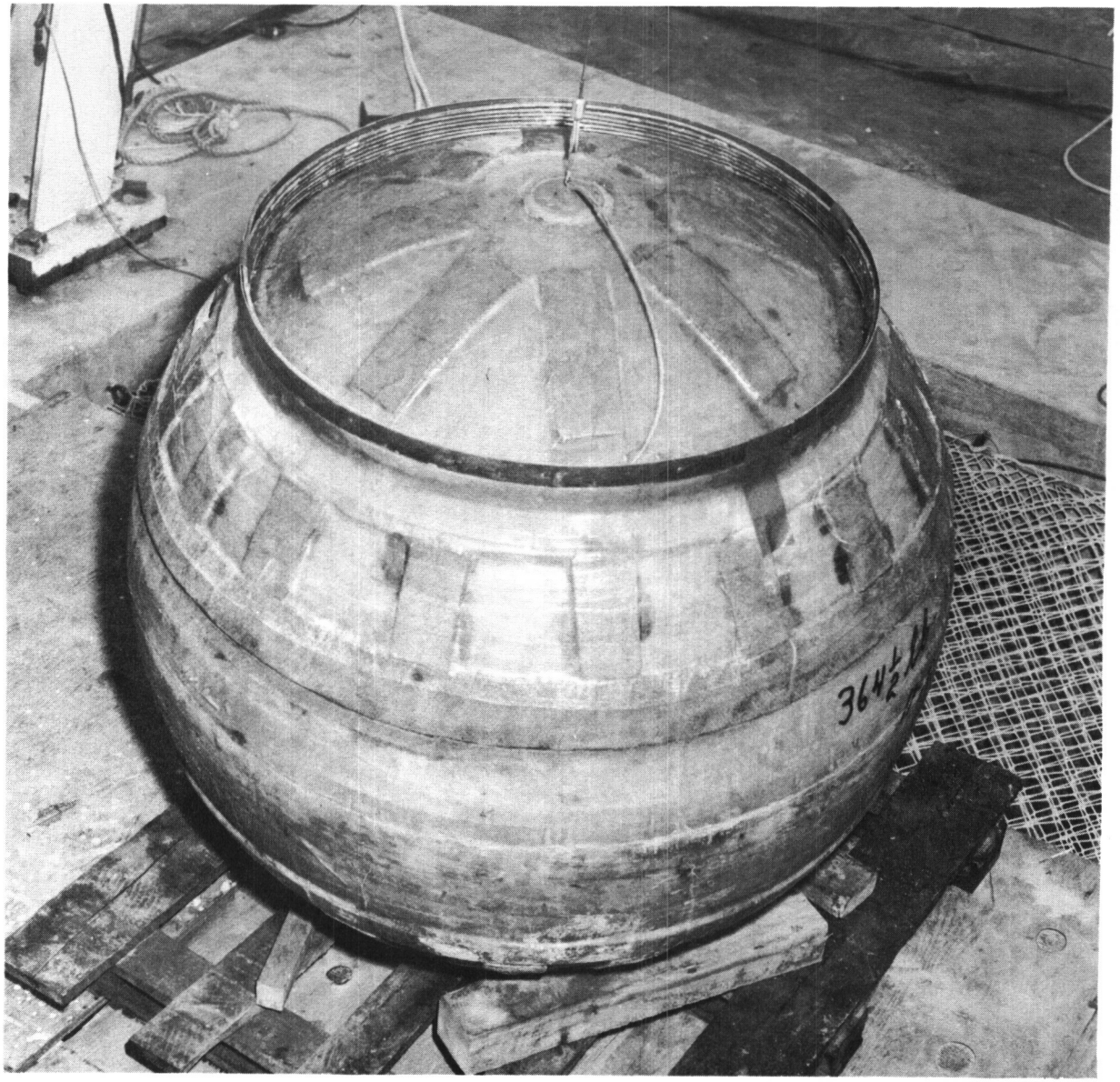

FIGURE 2-10 45-INCH FIBERGLASS SPHERE PROJECTILE

the projectile through the acceleration and air blast; and played out evenly. Due to weight the cable inertia and shock loads were of concern and this was handled by attaching the cable to a nylon bungee cord.

The solution appears very logical in retrospect. However, isolating and solving the problems was fierce and required quite a bit of test sampling to deduce. A summary of the instrumentation test configuration and result is shown in Figures 2-11, 2-12, 2-13, 2-14 and 2-15.

TEST NO.	1	2	3
DATE:	21 July 1966	22 July 1966	28 July 1966
Projectile Diameter Nominal Weight Shape	 45" 296 Disc	 45" 302 Disc	 45" 309 Disc
Accelerometer Pressure	50 psig	86 psig	116 psig
Terminal Speed(ft/sec)	308 ft/sec	400 ft/sec	474 ft/sec
Terminal Pitch Angle	---	---	---
Fuse-Link	3/16" Braided Nylon	3/16" Braided Nylon	3/16" Braided Nylon
Signal Cable	1 Belden 8434 1 Gulton C5HT	1 Belden 8434 1 Gulton C5HT	1 Belden 8434 1 Gulton C5HT
Cable Tether	3/32" Braided Nylon	3/32" Braided Nylon	3/32" Pref. Steel A/C
Tether/Cable Ties	Lacing Cord @ 6" Intervals	Lacing Cord @ 6" Intervals	None
Cable Jacket	None	None	1/2" PVC Tubing
Cable Layup	Spiral out to in	Spiral out to in	Spiral out to in
Cable to Projectile Hold-Down	Green Tape	Green tape	Green Tape
Cable Noise Level (Peak to Peak	Beldon 30 g Gulton < 10 g	---	---
Position of Leading Edge of Projectiles at time of Cable Failure	Impact + 35 ms	4 ft Inside Muzzle	6 ft Inside Muzzle
Probable Cause of Failure	---	Cable tangle from gas turbulance or interference from fuse remnant or insufficient wire slack on nylon tether.	Cable tangle from gas turbulance or interference from fuse remnant or cut by wire rope tether.
Remarks			

FIGURE 2-11

INSTRUMENTATION DEVELOPMENT TESTS 1 TO 3

TEST NO.	4	5	6
DATE:	3 August 1966	5 August 1966	25 August 1966
Projectile Diameter Nominal Weight Shape	 45" 315 Disc	 45" 309 Disc	 45" 300 Sphere (plywood)
Acceleration Pressure	118 psig	116 psig	110 psig
Terminal Speed (ft/sec)	508 ft/sec	447 ft/sec	462 ft/sec
Terminal Pitch Angle	---	45°	---
Fuse-Link	3/16" Braided Nylon	3/16" Braided Nylon	1/16" Steel A/C
Signal Cable	1 Belden 8434 1 Gulton C5HT	1 Belden 8434 1 Gulton C5HT	1 Belden 8434 1 Gulton C5HT
Cable Tether	3/32" Braided Nylon	7/32" Braided Nylon	1/8" 7x19 Pref. A/C
Tether/Cable Ties	Green Tape	Green Tape	None
Cable Jacket	None	None	No. 4 Thermofit
Cable Layup	Zig-Zag Across Top	Tight Spiral, in to out	Tight Spiral, out to in
Cable to Projectile Hold-Down	15# Cotton Ties on "U" Nails ea. 7"	15# Cotton Ties on "U" Nails ea. 4"	20# Cotton Ties on "U" Nails ea 4"
Cable Noise Level (Peak to Peak)	---	---	---
Position of Leading Edge of Projectile at Time of Cable Failure	At Muzzle	Before First 4 ft of Motion	2 ft of Stroke
Probable Cause of Failure	Cut by cotton ties or fuse remnant + excess whipping & tensile loads + edge of muzzle.	Cut by fuse remnant or cotton ties.	Cut by fuse remnant.
Remarks			

FIGURE 2-12

INSTRUMENTATION DEVELOPMENT TESTS 4 TO 6

TEST NO.	7	8	9
DATE:	30 August 1966	31 August 1966	7 October 1966
Projectile Diameter Nominal Weight Shape	45" 55.6 Disc (Foam)	45" 65.3 Disc (Foam)	45" 330 Disc
Acceleration Pressure	25 psig	50 psig	85 psig
Terminal Speed (ft/sec)	341 ft/sec	---	430 ft/sec
Terminal Pitch Angle	20°	---	15°
Fuse-Link	3/32" Braided Nylon	3/32" Braided Nylon	1/16" 7x7 Steel A/C
Signal Cable	Belden 8434	Belden 5434 and RG 174/U	Amergraph 4H219B
Cable Tether	None	1/8" 7x19 A/C	(Part of Sig Cable)
Tether/Cable Ties	---	None	---
Cable Jacket	None	No. 4 Thermofit	(Steel-Part of Sig Cable)
Cable Layup	Spiral in to out	Out to in spiral	Fig. 8 on Coil Forms
Cable to Projectile Hold-Down	None	1" Urethane Foam	Epoxy Coating
Cable Noise Level (Peak to peak)	---	---	---
Position of Leading Edge of Projectile at time of Cable Failure	12 ft out of muzzle	---	17 ft out of muzzle
Probable Cause of Failure	Cable tangle from gas turbulance and wrong spiral sense.	Projectile disintegrated in barrel.	Whip-lash in breech and sharp corner from broken conduit.
Remarks			Rigid anchor at trailer end of instrument cable.

FIGURE 2-13

INSTRUMENTATION DEVELOPMENT TESTS 7 TO 9

TEST NO.	10	11	12
DATE:	11 October 1966	21 October 1966	21 October 1966
Projectile Diameter Nominal Weight Shape	 45" 318 Sphere (Perlite)	 45" 340 Sphere (Perlite)	 45" 335 Sphere (Plywood)
Acceleration Pressure	84 psig	108 psig	87 psig
Terminal Speed (ft/sec)	385 ft/sec	437 ft/sec	396 ft/sec
Terminal Pitch Angle	---	---	---
Fuse-Link	1/16" 7x7 Steel S/C	1/16" 7x7 Steel A/C	1/16" 7x7 Steel A/C
Signal Cable	Belden 8434 and RF 174/U	Amergraph 4H219B	Amergraph 4H219B
Cable Tether	1/8" 7x9 Steel A/C	(Part of Sig Cable)	(Part of Sig Cable)
Tether/Cable Ties	None	---	---
Cable Jacket	No. 4 Thermofit	(Steel-Part of Sig Cable)	(Steel-Part of Sig Cable)
Cable Layup	Spiral out to in	Fig. 8 on Coil Forms	Fig. 8 on Coil Form
Cable to Projectile Hold-Down	1/4" Urethane Foam	Epoxy Coating	Epoxy Coating
Cable Noise Level (Peak to Peak)	---	$\approx$ 100 g S + N	---
Position of Leading Edge of Projectile at Time of Cable Failure	6 ft Out of Muzzle	---	8 ft Out of Muzzle
Probable Cause of Failure	Whip-Lash tension plus muzzle edge.	Projectile disintegrated in barrel.	Whip-lash plus rigid anchor.
Remarks	---	Rigid anchor at trailer end of instrument cable.	Rigid anchor at trailer end of instrument cable.

FIGURE 2-14

INSTRUMENTATION DEVELOPMENT TESTS 10 TO 12

TEST NO.	13	14	15
DATE:	27 October 1966	2 November 1966	23 November 1966
Projectile Diameter Nominal Weight(lbs) Shape	 45" 307 Disc	 45" 330 Disc	 45" 364 Fiberglass Perlite
Acceleration Pressure	86 psig	85 psig	95 psig
Terminal Speed (ft/sec)	430 ft/sec	394 ft/sec	---
Terminal Pitch Angle	---	5°	---
Fuse-Link	1/16" 7x7 Steel A/C	1/16" 7x7 Steel A/C	1/16" 7x7 Steel A/C
Signal Cable	Amergraph 4H219B	Amergraph 4H219B	Amergraph 4H219B
Cable Tether	Part of Sig Cable	Part of Signal Cable	Part of Sig Cable
Tether/Cable Ties	---	---	---
Cable Jacket	(Steel-Part of Sig Cable)	(Steel-Part of Sig Cable)	(Steel-Part of Sig Cable)
Cable Layup	Fig. 8 on Coil Form	32" Dia Cyl Coil	32" Dia Cyl Coil
Cable to Projectile Hold-Down	Epoxy Coating	Epoxy Coating	Epoxy Coating
Cable Noise Level Peak to Peak	---	---	---
Position of Leading Edge of Projectile At Time of Cable Failure	5.2 ft Out of Muzzle	Continuity Throughout Event	Continuity Throughout Event
Probable Cause of Failure	Whip-lash plus breech guide.	Success	Ball broke up during acceleration
Remarks	10'X1/2" Nylon line, elastic anchor at trailer end of the instrument cable.	Tension on nylon line 600 lb peak.	---

FIGURE 2-15

INSTRUMENTATION DEVELOPMENT TESTS 13 TO 15

SECTION 3

BALSA SPHERE DESIGN AND FABRICATION

The basic requirement of the balsa wood limiter is that it provide omni-directional impact protection for an internal spherical payload. Since balsa has grain oriented properties it is necessary that the spheres be constructed with radially oriented grain to achieve optimal material efficiency. This requires a sphere constructed of small segments. In addition, these segments must be developed in a precise geometric form for proper assembly into a spherical shape. The basic geometry is discussed early in the following section. Subsequent sections discuss in detail the fabrication and assembly methods developed to provide an integral package of payload and limiter. A pictorial of the complete assembly sequence is shown in Figure 3-1.

3.1 LIMITER DESIGN

It was a design requirement that the spherical balsa wood impact limiter be fabricated such that the maximum angular difference between the grain and the radius vector never exceeds 15 degrees. A second requirement relates to the maximum saw cut depth required to fabricate each segment; this could not exceed 13 inches to allow utilization of the specially purchased 32 inch diameter circular saw which represents the maximum size acceptable to achieve the required precision cuts. A further constraint was to minimize fabrication and assembly costs by manufacturing the limiter out of a minimum number of different detail blocks. The first two requirements dictate that the previous method of construction utilized for Ranger (an icosahedron of 20 trisected tetrahedrons, see Figure 3-2) is not acceptable, since it would produce a maximum off-radial grain orientation of 18.7 degrees, and would result in a depth of cut requirement (for a 45-inch diameter) unacceptable to state-of-the-art equipment.

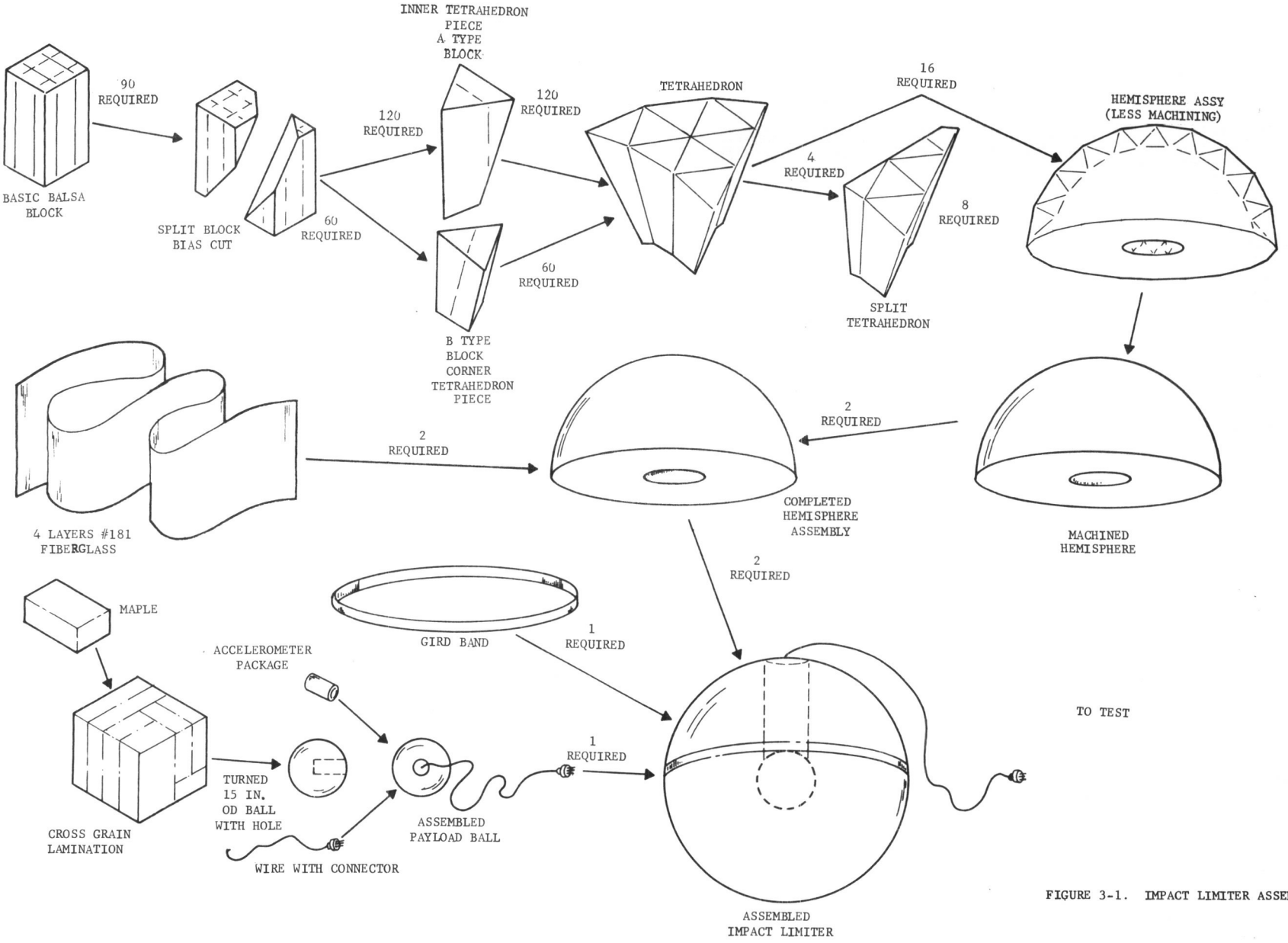

FIGURE 3-1. IMPACT LIMITER ASSEMBLY SEQUENCE

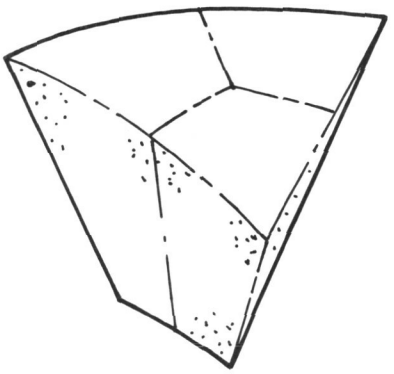

FIGURE 3-2

TRI-SECTED TETRAHEDRON

The elimination of this method of construction also eliminated any possibility of assembling the impact limiters from identical blocks. The geometry of a spherical surface dictates that the sixty pieces (20 tri-sected tetrahedrons) from which the Ranger limiters were constructed is the maximum number of identical pieces which can be assembled into a sphere. Thus, to reduce the maximum off-radial grain orientationto less than 15^{o} and reduce the depth of cut requirements. The limiters for this program were constructed from 180 segments of two types. The approach is illustrated in Figures 3-1 and 3-3. The completed spherical limiter contains 120 pieces of type "a" and 60 pieces of type "b" block. The bases of the "a" pieces are spherical isoceles triangles; these are assembled to form a hexagonal base to which the corner "b" segments are added to make a tetrahedron for subsequent assembly into an icosahedron. This design approach produces an impact limiter with a maximum of 13.97 degrees off-radian grain orientation. It possess an additional advantage over other 180 segment divisions in that it is composed entirely of three-sided pieces thus requiring a minimum of surface cuts.

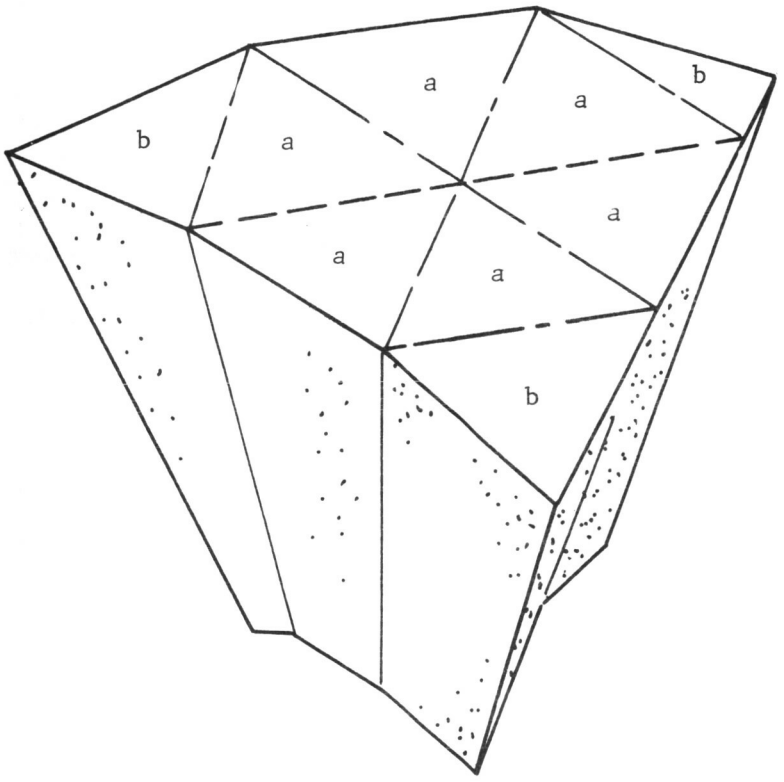

FIGURE 3-3.

NINE-SEGMENT TETRAHEDRON CONFIGURATION

3.2 LIMITER GEOMETRY

The geometry of the segments forming the tetrahedron from which the 20 sided icosohedron is constructed is shown in Figure 3-4. The configuration was evolved by "slicing off the corners" of the (rounded) tetrahedron shown in Figure 3-4 to form a regular hexagon on the spherical surface. This spherical hexagon was then subdivided into six identical pieces by dropping arcs from the hexagons geometric center (O', Figure 3-4) to its vertices. The geometrius of the two resulting segment types are shown in Figures 3-5 and 3-6. In each case, the geometry is presented in relation to the center of an inscribed right circular cone whose axis forms the center of rotation for the raw block machining fixture (See Paragraph 3.3). The maximum off-radial grain angles of the two basic detail blocks are as follows:

Inner Tetrahedral Segment	13.97 degrees
Corner Tetrahedral Segment	13.11 degrees

3.3 SEGMENT FABRICATION

The geometry of the two configurations of detail balsa wood blocks was achieved in two stages. The basic raw material block was first held in a fixture, and parted with a bias saw cut performed on a standard band saw. Next, the unfinished detail block was placed in an indexing fixture and all three precision cuts made with a traveling circular saw. A Rodgers radial saw utilizing a 32-inch diameter carbide tipped circular saw blade was purchased for this task. It provided a 13 depth of cut with a horizontal cutting stroke of 36-inches. The saw and fixture are shown in Figure 3-7. Final manufacture of the pieces is accomplished by installing the split balsa block in a holding fixture which rotates the part about the axis of a right circular cone inscribed in the defined segment. The selection of this axis of rotation (coincident with the nominal grain direction) dictates that the dihedral angle of each side relative to the base is identical. Thus, the cutting of each segment is accomplished by orienting the fixture axis at a fixed angle (α, Figure 3-8) relative to the direction of saw blade motion and proceeding through three successive sawing and rotational indexing operations. The angle α is set once for each type of segment and is equal to the half angle of the right circular cone inscribed in the segment.

Experience has clearly demonstrated that the success of the subsequent tetrahedron and hemisphere assembly operations is directly dependent upon the surface finish and dimensional accuracy obtained in the aforementioned sawing operation. The surface finish of the segment was controlled by the rigidity and travel rate of the traversing saw head and the speed and grind of the saw blade; the dimensional accuracy was controlled by the quality, rigidity and accuracy of the tooling.

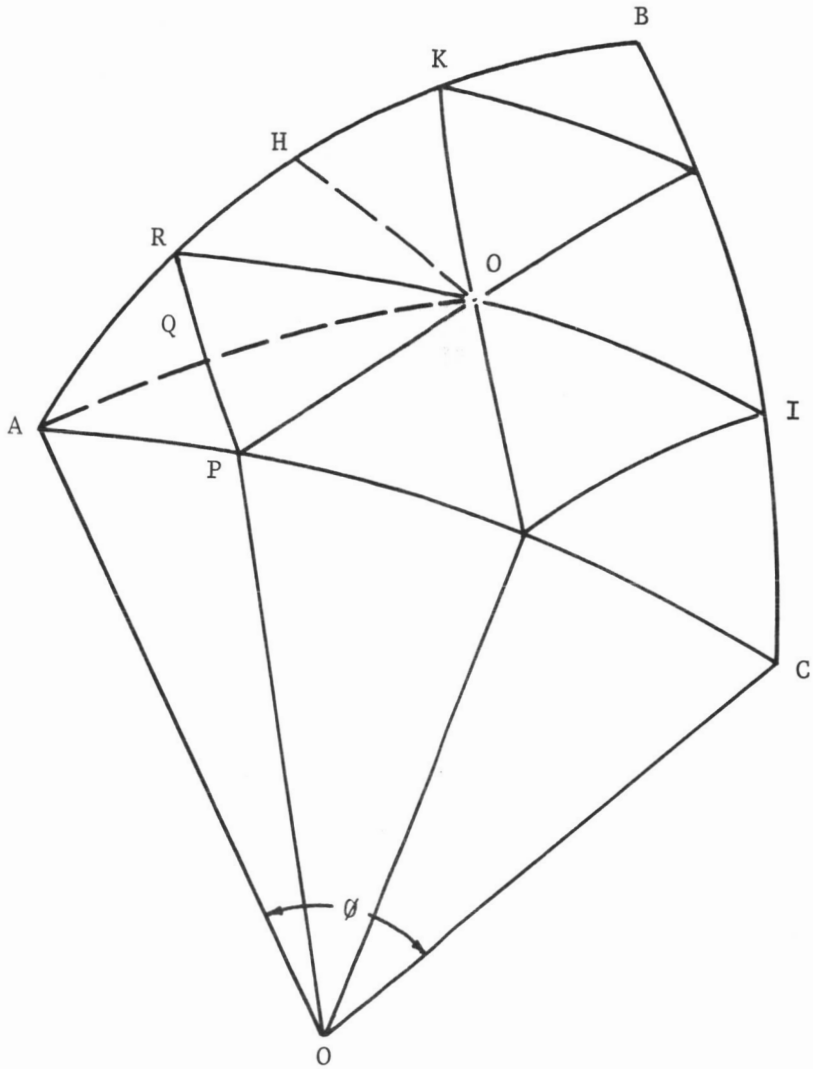

FIGURE 3-4

TETRAHEDRON SEGMENT GEOMETRY

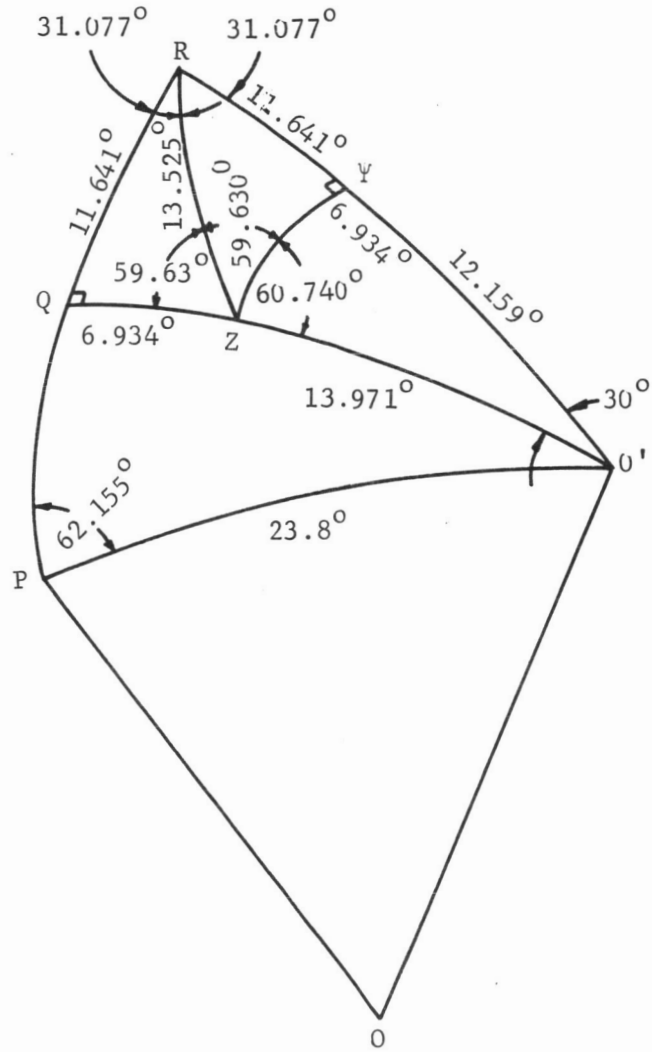

FIGURE 3-5

INNER TETRAHEDRAL SEGMENT GEOMETRY

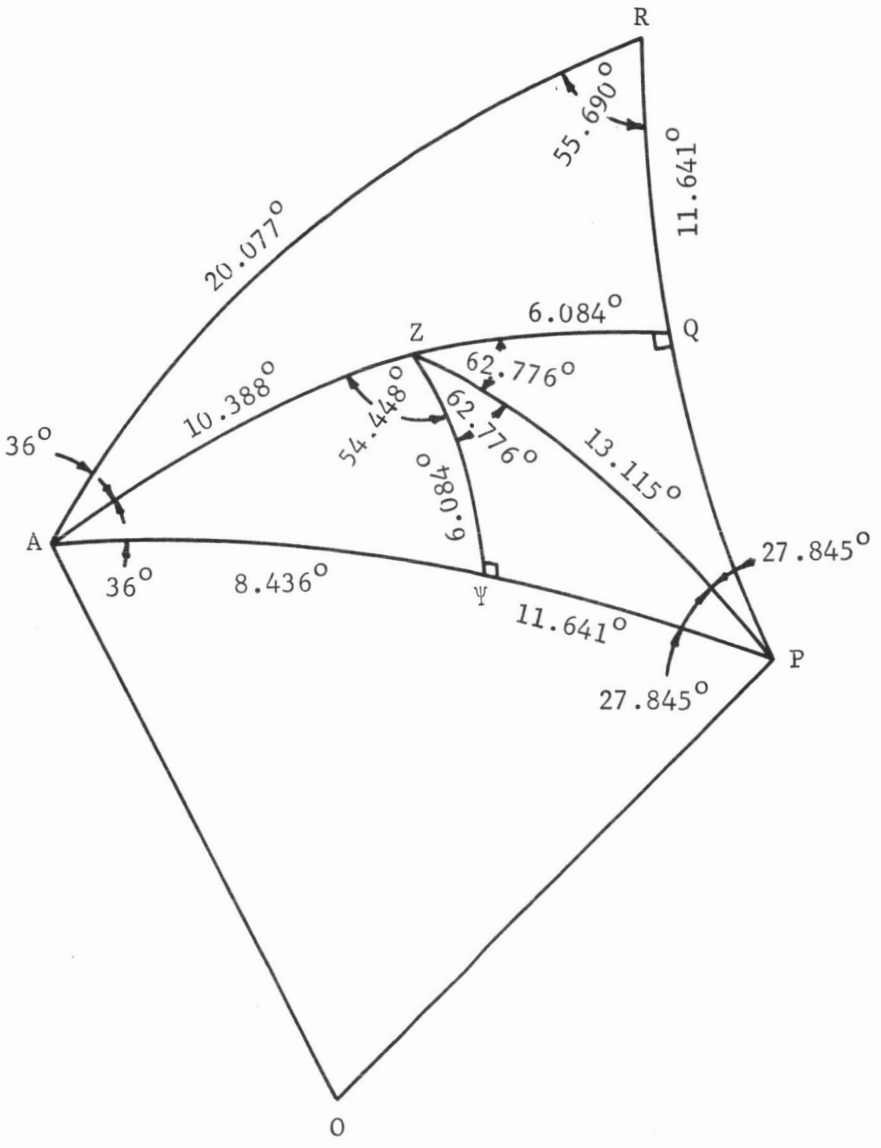

FIGURE 3-6

CORNER TETRAHEDRAL SEGMENT GEOMETRY

FIGURE 3-7 BALSA SEGMENT SAW

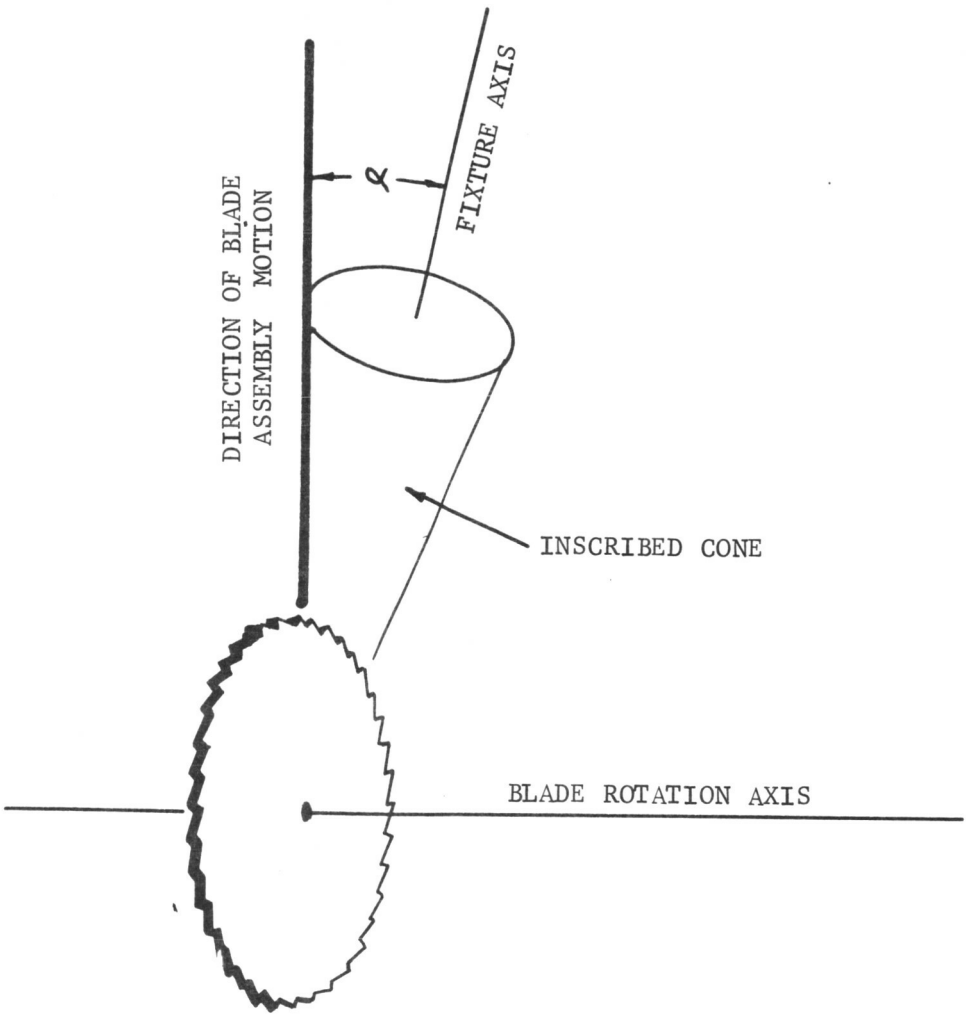

FIGURE 3-8

SCHEMATIC OF CUTTING GEOMETRY

The surface finish on the segments was excellent and the angular geometry was controlled to within 0.004 inches in 15 inches of length. Thus, accurate mating of the segments in the tetrahedron assembly was assured. The completed balsa segments are shown in Figure 3-9.

3.4 TETRAHEDRON AND HEMISPHERE ASSEMBLY

The balsa segments were then placed into a tetrahedron holding fixture. A .005-inch maximum glueline was obtained with a combination of vacuum bag curing and the mechanical holding fixture. The mating surfaces of the tetrahedral segments were first coated with the Epon 828/Epocast 985 resin system and then mated in the assembly fixture as shown in Figure 3-10. It is essential that the side surfaces ofthe assembly are smooth to permit accurate assembly of the hemisphere and minimize resin content. Therefore, extensive care was taken to accurately mate the edges of the tetrahedral segments. As shown in the photo, the visible edges of the first six segments were aligned first and then the last three inner segments moved into their final position.

After all segments were in place, uniform pressure from mechanical clamps was applied to the top of each segment. Then a hard vacuum was applied for four hours to cure the resin. Twenty tetrahedron assemblies are used in each impact limiter sphere.

The sphere is built-up from two independently assembled and machined "half-icosahedron" sub-assemblies. These latter sub-assemblies are built-up from eight full tetrahedron assemblies and two split tetrahedron assemblies in the following manner:

(1) A trial assembly of the pieces is made on a large flat surface table.

(2) After coating all bond surfaces with adhesive, the base pieces (two full tetrahedrons and four splits) forming the equatorial section of the hemisphere are assembled to form a ring.

(3) A piece of PVA tape is tied around the base of the ring to prevent any large movement of the parts.

(4) The remainder of the segments are added to complete the hemisphere andsurfaces are covered with perforated PVA film and bleeder cloth as necessary.

(5) A vacuum bag is installed over the assembly, and sealed to the table and a vacuum of 3 to 5 inches is pulled

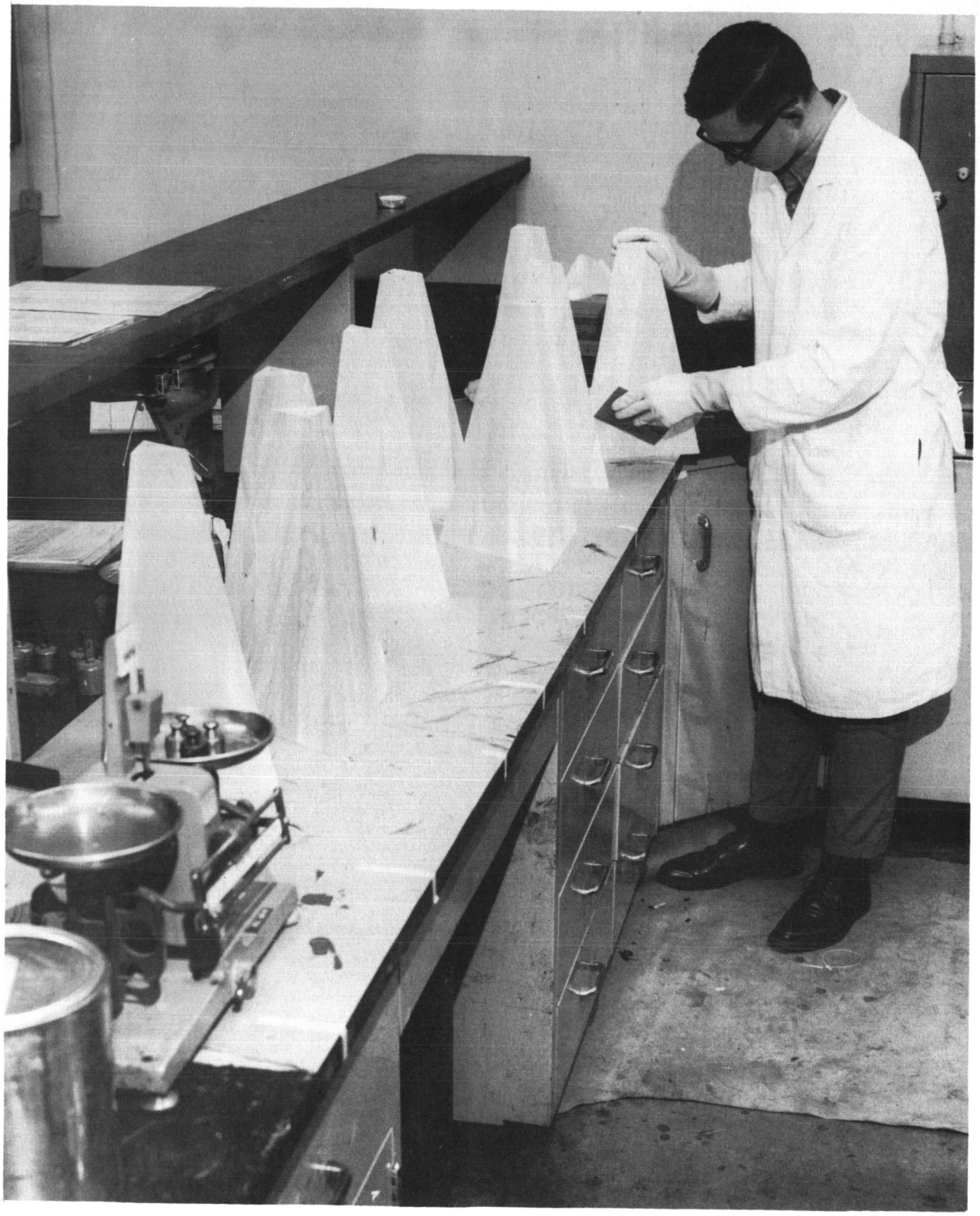

FIGURE 3-9 COMPLETED BALSA SEGMENTS

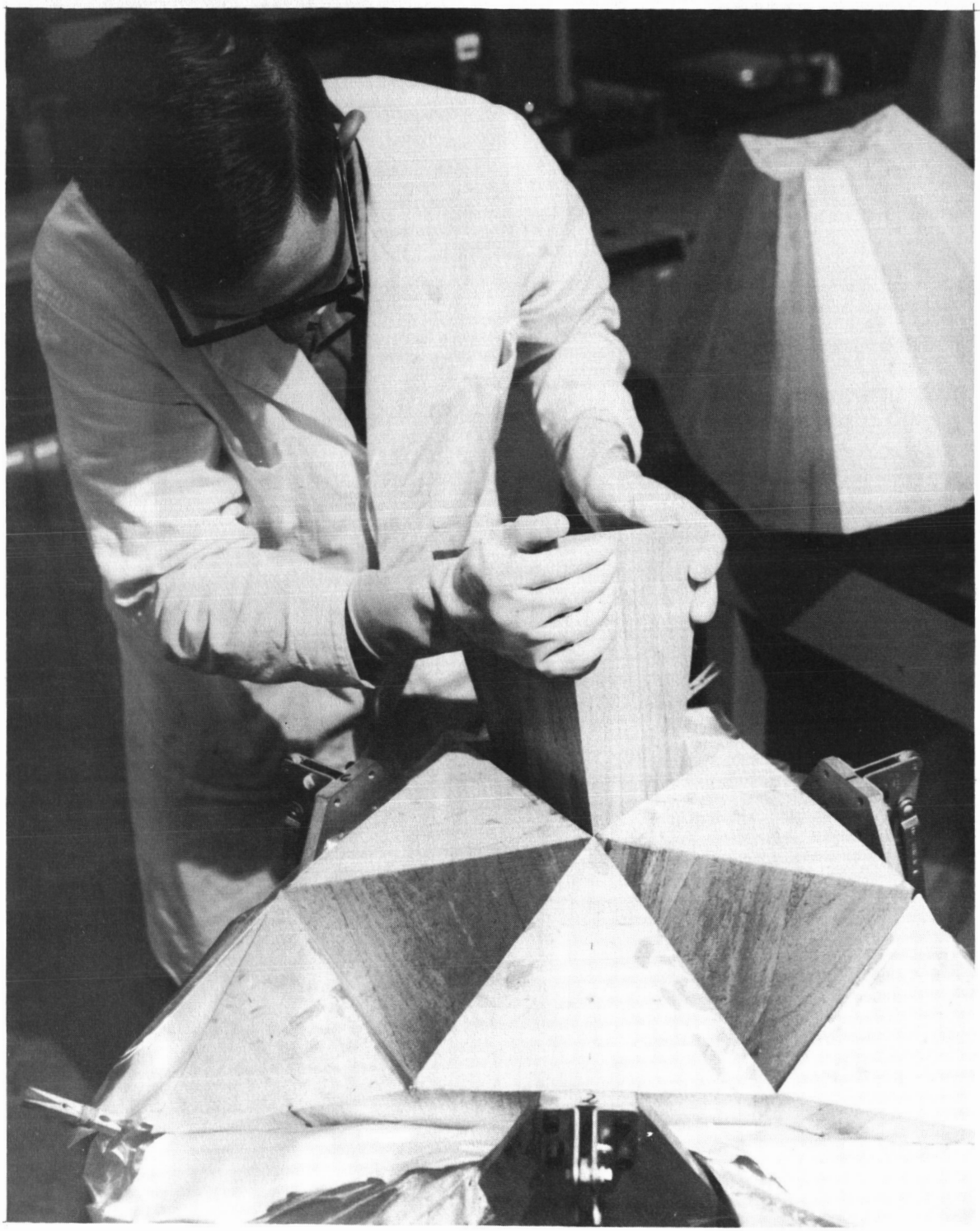

FIGURE 3-10 TETRAHEDRON ASSEMBLY

(6) While under the light vacuum, the individual segments are waltzed back and forth until a uniform fit is obtained between all the parts.

(7) A vacuum of 27 to 29 inches is pulled and the assembly is cured for 12 hours. A vacuum is maintained at all times.

(8) After cure and inspection, the part is transferred to the shop for the contour operation.

To complete the final hemisphere configuration the bonded subassembly is routed to the Machine Shop for two fixtured operations consisting of a combined facing and 15-inch ID contour bore followed by a 45-inch diameter spherical radius of the exterior surface. These surfaces are generated by the substitution of a very high speed motor-driven radiused carbide cutter for the normal single-point tool. The dimensional accuracy of the two spherical radii controlled by precision follower templates mounted on the 56-inch Giddings and Lewis vertical turret lathe. This machine tool is equipped with a 360-degree Minneapolis-Honeywell electrical-hydraulic tracing unit to permit extremely close tolerance work. The surface finishes resulting from this technique require little or no hand finishing. The operation is shown in Figure 3-11.

3.5 INNER PAYLOAD

The 15-inch diameter inner payload was required to have a density of 50 to 60 lb/ft^3 and possess sufficient structural integrity to resist any permanent deformation from impact. It was additionally required to house the accelerometer required to measure the deceleration time history of impact.

The payload was constructed of a hard maple wood possessing the specified density characteristics. Fabrication was accomplished by laminating a 15-inch block from 1 to 2 inch thick blocks laid at 90 degrees to each other in the manner of plywood. This block was then turned to the specified 15-inch diameter.

The payload was constructed of maple with an aluminum ballast plate at its center. The latter allowed the payload to achieve the proper weight (approximately 50 pounds) and provided a mounting surface for attachment of the instrumentation. Fabrication was accomplished by laminating a block from 1 to 2 inch thick, 90 degree pie-shaped segments, with the seams of successive layers displaced 90 degrees for added strength. This block was then turned to the specified 15-inch diameter and a radial access provided to its center for installation of instrumentation (a matching radial hole was also provided in the upper limiter half).

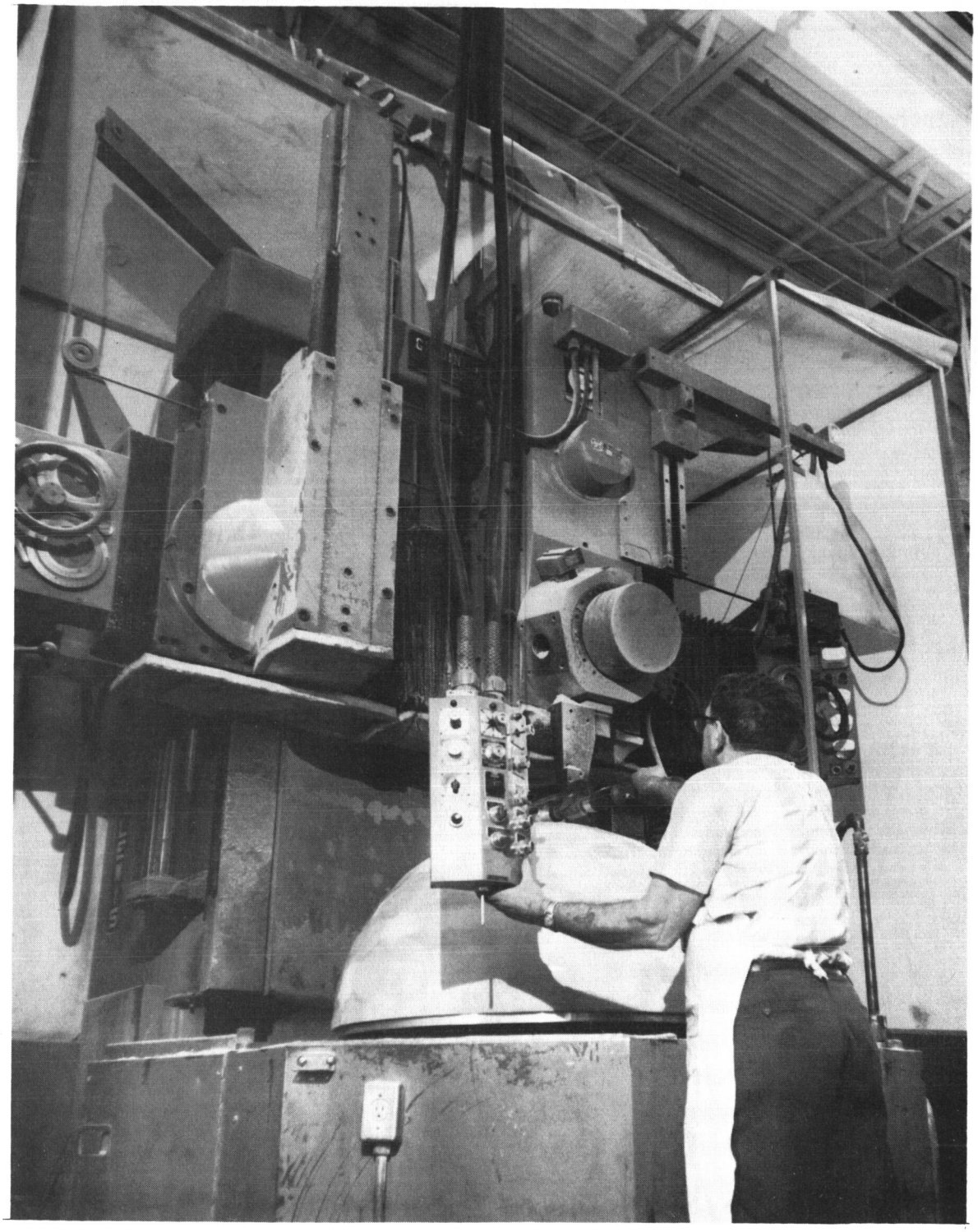

FIGURE 3-11 MACHINING BALSA HEMISPHERES

3.6 EXTERNAL COVER

An external cover was provided for the limiter to (1) prevent loss of moisture, (2) increase impact strength; (3) prevent loss of balsa sections during primary impact; and (4) provide abrasion resistance for sliding impacts.

The cover was constructed from four layers of #181 fiberglass cloth impregnated with an Epon 828/985 resin system. The material was applied to the hemispheres one layer at a time (as a single piece) and then draped into position by the use of a serrated squeegees.

3.7 MOISTURE CONTENT

It was a design requirement that the nominal moisture content of the balsa wood sphere be reduced from its natural 8 percent level to 2 $\pm$ 1 percent prior to test in order to maximuze the specific energy absorption capability of the material.

A series of sample tests conducted by Philco-Ford early in the limiter fabrication phase established that small balsa samples covered with a four layer fiberglass cover gave up moisture almost as rapidly as non-covered balsa when subjected to a hard (30 inch) vacuum and 120°F. In addition, it was determined that at ambient conditions the four layer fiberglass cover specified in the Philco-Ford design was adequate to maintain the balsa moisture content at 2 $\pm$ 1 percent for what was later established to be a period of at least six months. It was therefore concluded that positive control of the final assembly moisture content could be achieved by drying the assembled and covered sphere in a 120°F vacuum environment.

This method of moisture reduction was applied to the first impact limiter assembled (S/N #1): the results were unsuccessful. The sphere was placed in a vacuum bag at 120°F for 162 hours with no appreciable loss in weight. It was then moved to a BEMCO Altitude-Temperature Chamber where a harder vacuum of .46 mm Hg was applied at 120°F for six hours. Again there was no reduction in weight. Thus, at test the S/N #1 sphere moisture content remained at a nominal 8 percent.

The moisture control procedure was altered for S/N #2. After the hemispheres were covered, but before final assembly, they were placed in a vacuum bag at 120°F. After 64 hrs only 1.1 percent moisture had been removed. The hemispheres were then placed in the BEMCO Chamber at 120°F and a vacuum varying between 1 and 3 mm Hg applied. There was no moisture trap between the chamber and the compressor. Hence the water contaminated the oil and reduced the efficiency of the chamber; during the 46 hrs in the BEMCO, the oil was changed twice to maintain the hard vacuum condition. During this period 3.5 percent was removed from each hemisphere. Removal of the moisture resulted in a shrinkage of the S/N #2 hemispheres. The

internal diameter was reduced from 15 in. to about 14.80 in., and the outer diameter from 45 in. to about 44.75 in. Accordingly, the balsa volume of a hemisphere was reduced from 13.3 ft^3 to about 13.0 ft^3 and the circumference of the sphere was reduced by 0.8 in. The shrinkage also resulted in slight puckering of the covers over the surface of the hemispheres.

To reduce the cover deformation and drying time, the moisture control procedure was further altered for the S/N #3 sphere assembly. The moisture control procedure was altered further for S/N #3. After the hemispheres were machined, they were placed in the BEMCO at 120°F and at a vacuum varying between 1 and 3 mmmHg. A total of about 6 percent moisture was removed from each hemisphere during the first 40 hrs in the chamber. These hemispheres also shrunk during the moisture conditioning. The internal diameter was reduced to 14.88 in., the outer diameter to 44.78 in., and the hemisphere balsa volume to 13.2 ft^3.

After moisture conditioning the S/N #3 hemispheres were placed in vacuum bags until the covers were installed. No moisture re-entered the wood during this period of 69 hrs. During cover assembly it was noted that the first coat of resin, applied before the first fiberglass layer, was readily absorbed by the wood. About 2 lbs of resin in excess of that normally used in the cover assembly were consumed on each hemisphere.

After cover assembly, Silica Gel was placed in the cavity of each hemisphere and the exposed balsa was sealed with polyethylene sheeting. Final assembly proceeded in accord with section 28.

It should be noted that for each sphere the amount of moisture to be removed was determined by the removal of four small sample cores at 90° positions on the equatorial surface of the unassembled hemispheres. These cores were weighed, dried at 250°F $\pm$ 5°F for 12 hrs, and re-weighed to establish the moisture content of the wood immediately prior to the demoisturization processing. The cores were then bonded into their original position before final assembly proceeded.

An additional problem which occurred and caused great difficulty during the final assembly process was the distortion, minor swelling and warpage which appeared on the inner hemispherical and equatorial surfaces of the balsa following moisture conditioning. This impaired the precise fit provided for the internal spherical payload during machining. For this reason the moisture conditioning of the S/N #4 sphere was eliminated to allow development of an independent solution to the cover design and bond problems which arose during the first three tests.

No splitting of balsa during or after moisture conditioning of the first three spheres was observed.

A summary of the results of moisture conditioning is shown in Table 3-1.

TABLE 3-1

MOISTURE CONTROL - S/N #1, #2 AND #3

Serial Number	Weight Before Conditioning (lbs)	Moisture Content Before Conditioning (%)*	Time In Att. - Temp. Chamber (Hours)	Moisture Loss During Conditioning (%)	Weight After Conditioning (lbs)	Moisture Content After Conditioning (%)
1 (Sphere)	336.6	8.0 $\pm$ .6	170 **	0	336.6	8.0
2-1 (Bottom)	126.5	7.2 $\pm$ .6	110 ***	4.6	120.7	2.6
2-2 (Top)	127.0	6.5 $^{+\ .5}_{-\ .8}$	110 ***	4.6	121.2	1.9
3-1 (Bottom)	122.8	7.6 $^{+\ .5}_{-\ 1.2}$	40	5.8	115.7	1.8
3-2 (Top)	122.3	7.6 $^{+\ .7}_{-\ 1.4}$	40	6.1	114.8	1.5
4 NO MOISTURE CONDITIONING						

* The moisture content of the hemispheres prior to conditioning is established by removing four small samples (0.1 to 2 grams each) from the equatorial surface of the balsa and drying the samples at 250°F for 12 hrs. On S/N #1 and #2 all samples were within a range of $\pm$ 13 percent. On S/N #3-1 and 3-2 one sample in each hemisphere exhibited a moisture content 1.4 percent and 2.2 percent respectively less than the average of the other three samples. The samples are bonded back into the hemispheres before final assembly.

** The completely assembled S/N #1 was placed in a vacuum bag identical to those used in curing balsa assemblies and in a temperature environment of 120°F. After 120 hrs no moisture had been removed. The sphere was then placed in the BEMCO chamber at 120°F and a vacuum of .46 mm Hg for 6 hrs.

*** The S/N #2 hemispheres were initially placed in vacuum bags and in a temperature environment of 120°F. After 64 hrs only 1.1 percent moisture had been removed. The hemispheres were then placed in the BEMCO Chamber. The remaining 3.5 percent moisture was driven off in 46 hrs. A lack of pressure rise during the last 8 hrs indicated that little if any additional moisture was being driven off and the hemispheres were removed from the chamber.

3.8 FINAL LIMITER ASSEMBLY

The final assembly operation consists of bonding the spherical wooden payload into the matched limiter halves; bonding the equatorial limiter surfaces together; and finally placing a band around the parting line.

Installation of the payload and bonding of the limiter halves was performed as a single step. The payload was first lightly sanded and cleaned with M.E.K. All surfaces to be joined were then coated with an excess of adhesive to account for any minor mismatching of mating parts and the pieces assembled into their respective positions. An equatorial bleeder cloth was then placed around the parting line and the entire assembly installed into a vacuum bag for the duration of the room temperature cure.

The equatorial bond for formed by four 8-in. wide strips of epoxy impregnated glass cloth. This in turn was covered with a layer of perforated PVA followed by several layers of bleeder cloth. All were held in place by a wrapping of PVA tape. It was then again vacuum bagged and cured.

The hemisphere and payload are shown in Figure 3-2.

3.9 DESIGN IMPROVEMENTS IN SPHERE NO. 4

The first three balsa spheres were constructed in parallel, as previously described, prior to the commencement of test. Conversely, the S/N #4 balsa sphere was only constructed to the machined hemisphere stage at test initiation; the cover had not been installed nor had the final assembly operation been committed. This allowed design improvements to be made in the final spheres' assembly procedures and materials based on observations of the first three tests. The two basic observations noted were:

(1) The payload had separated from the balsa seat. A substantial amount of bond area on the sphere did not develop strength equal to that of the balsa. Thus, improving the total bond strength and area could raise the payload separation threshold levels thereby improving limiter performance.

(2) The exterior fiberglass cover experienced multiple tears during impact of the sphere. The tear strength of the cover was found to be very low once started.

As a result of these observations sample tests were conducted to seek improvement in payload bonding and cover tear resistance.

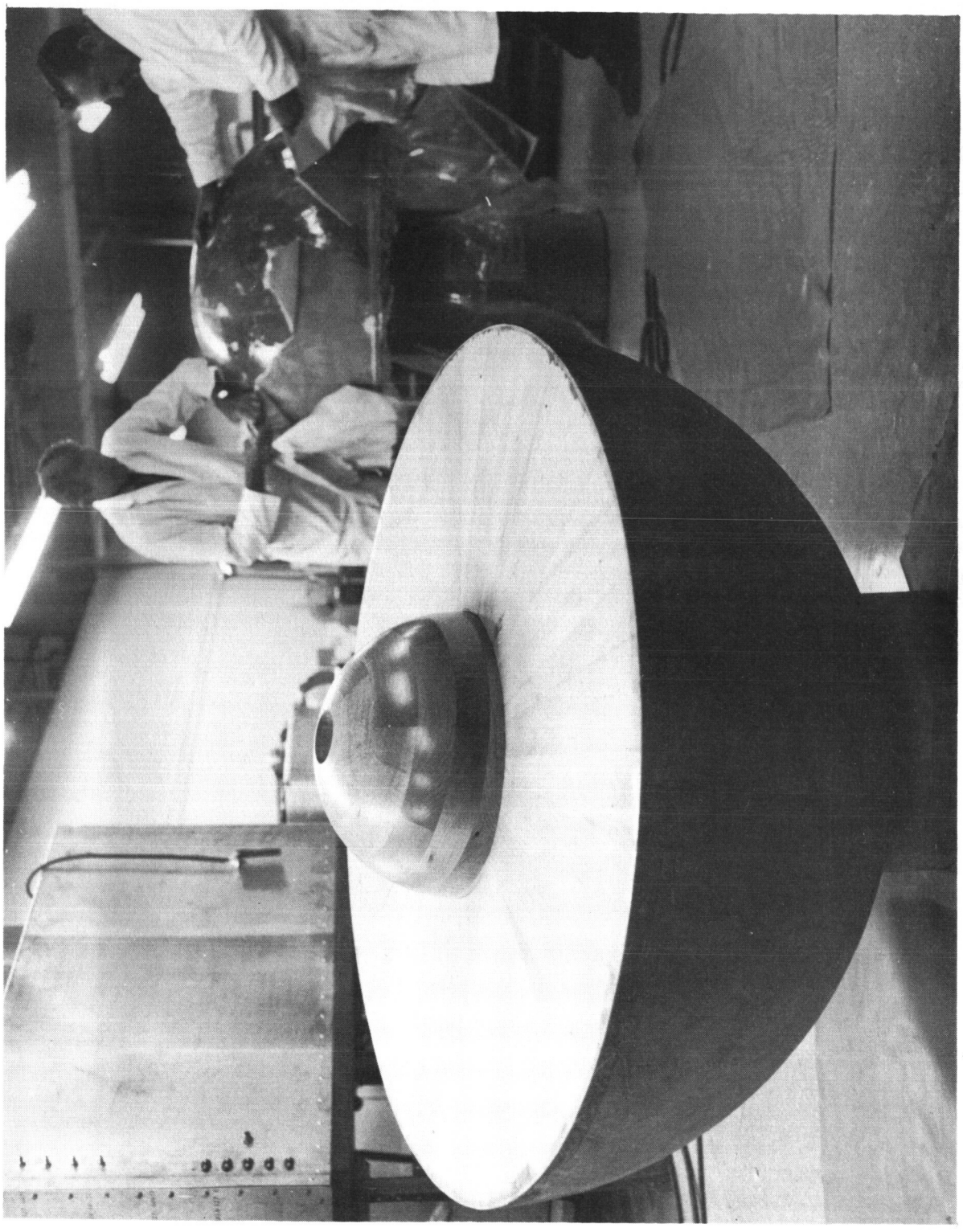

FIGURE 3-12 PAYLOAD AND HEMISPHERE ASSEMBLY

The following changes were incorporated into the payload bond process. The payload was roughed with No. 60 sand paper and cleaned with M.E.K. A new adhesive system utilizing EPON 828 resin - Versamide 140 hardener was incorporated. This was used diluted as a primer for both the payload and the balsa surfaces and undiluted as the final adhesive. An excess resin puddle was placed in the balsa seat prior to assembly to avoid entrapment of air and the hemispheres were installed to the payload independently to assure a sound joint.

The cover was changed to a tougher material and resin to increase tear resistance while still maintaining reasonable tensile strength. A two-layer nylon cloth and urethane resin cover of approximately equal weight to the previous cover was installed. The cloth material was ballistic nylon 34163 manufactured by J. P. Stevens. This material had poor drape qualities and a segmented cover was required. Six segments on each hemisphere and on equatorial band was used.

SECTION 4

BALSA SPHERE TEST PROGRAM

4.1 TEST REPORT ON SERIAL NOS. 1, 2, AND 3 BALSA SPHERES

4.1.1 ABSTRACT

Three 45-inch diameter balsa impact limiters were impacted against the reinforced concrete seismic block at speeds of 426, 365 and 378 ft/sec respectively. The programmed test velocities were met with the pneumatic accelerator facility. Instrumented data on velocity and acceleration was obtained for all tests. The peak impact acceleration was 6200, 4000, 3900 g respectively for each test. Payload impact protection was demonstrated at speeds of 365 and 378 ft/sec while the payload bottomed out and was damaged at 426ft/sec. Based on the Philco-Ford analytical model survival was expected to 378 ft/sec.

Associated with all impacts, even those where a full impact protected survival occurred, was the complete separation of the balsa limiter from the payload. An attempt was made to determine the possible causes of this phenomenon. An analysis of the payload cannonballing and the cover strength indicated these as positive contributive causes of balsa limiter break-up. The speculation is strong that with improved payload bonding and cover strength the survival impact level of the payload can be raised above the demonstrated levels.

4.1.2 SPECIMEN DESCRIPTION

The 45-inch diameter spherical test specimens were constructed of 9 lb/ft^3 balsa wood surrounding a 50 lb, 15 in. diameter, laminated maple payload with an accelerometer instrument package at the geometric center.

Each sphere was constructed in accordance with Aeronutronic Drawing SK25461 to provide a configuration with a balsa grain off-radial orientation of not more than 15 degrees. Hemispheres were built-up from 90 segments of two types. These segments were first assembled into ten 9-element, tetrahedral subassemblies, and then assembled into half-icosahedron assemblies. These peices were next precision machined into hemispheres in a 52 in. Giddings and Lewis vertical turret lathe in preparation for final assembly. The final assembly procedure utilized on each sphere was, however, slightly different due to the in-line development of a satisfactory approach to demoisturization.

On the S/N #1 sphere the fiberglass cover (consisting of four layers of fiberglass cloth and Epon 828/Epocast 985 Resin) was installed on the hemispheres prior to de-moisturization. The covered hemispheres were then bonded to the payload and a four layer fiberglass band applied to the equatorial joint. The completed assembly was then placed within a vacuum bag and held at 130°F for seven days in an unsuccessful attempt to withdraw the excess moisture through the cover (this had been achieved successfully with samples). The assembled sphere was then removed from the vacuum bag and placed in a vacuum chamber at 450 μ pressure and 140°F for another six hours in a further attempt to withdraw moisture. This also was unsuccessful. Thus, at test the sphere moisture content remained at 8 percent.

The cover was installed on the S/N #2 hemispheres in a manner similar to S/N #1. However, the de-moisturization was performed over a five-day period in a 140°F vacuum chamber prior to assembly onto the payload. This resulted in a shrinkage of the inside diameter of the limiter to 14.80 in. (from 15.00 in.) and in warpage of the equatorial plane. These factors severely hampered fit and adversely affected bond line thickness during the final stages of assembly.

On the S/N #3 limiter, drying of the hemispheres was accomplished in 40 hrs (at 140°F in a vacuum) by performing de-moisturization prior to cover installation. This again resulted in a shrinkage to a 14.88 in. of the limiter inside diameter and further aggravated warpage of the equatorial plane. It should also be noted that multiple changes of the vacuum pump oil were required in all cases to achieve the de-moisturization described.

4.1.3 TEST RESULTS

Table 4-I presents a summary of measured data. Motion picture coverage indicated that all three limiters left the gun nozzle with no discernable damage, tip-off or spin. No rebound was seen. Breech camera coverage gave no data for S/N #2 and S/N #3 due to dense water clouds from the acceleration gas chamber. Breech camera coverage for S/N #1 indicated normal cable action. Target area impact coverage gave no data for S/N #2 due to a dense water cloud around the projectile. No impact data were obtained for S/N #1

TABLE 4-I

Shot No.	Balsa Test No.	Date	S/N	Gross Weight*	Peak Acceleration	Speed	Peak Deceleration	Footprint Diameter
16	1	11/30/66	2	336 pounds	400 g	426 fps	6200 g	46 in.
17	2	12/09/66	3	331 pounds	300 g	365 fps	4000 g	42 in.
18	3	12/19/66	1	351 pounds	250 g	378 fps	3900 g	42 in.

*Including 6.5 lb instrumentation cable.

due to camera failure. By using a back-lighted technique, 6-1/2 milliseconds of photo data were obtained for S/N #3. The impact action was observed until the specimen had apparently come to rest and the crushed up flat one limiter diameter, but no break-up of the limiter was seen before the entire scene was obscured by the water cloud. The crush stroke could not be estimated with any accuracy from the films because the top of the ball was obscured by fog.

Figure 4-1 is a tracing of the oscillogram obtained from the S/N #2 test. The peak shock level was indicated as 6200 g, but reasonable smoothing of the data to discount structural ringing of the instrument package would yield a value closer to 5000 g. At 3-1/2 milliseconds after first contact, the trace goes off scale in a downward direction, probably due to a momentary short circuit between one power lead and one signal lead in the instrumentation cable.

Figure 4-2 is a tracing of the oscillogram obtained from the S/N #3 test. The peak shock level was indicated as 4000 g.

Figure 4-3 is a tracing of the oscillogram obtained from the S/N #1 test. The peak shock level was indicated as 3900 g. The data was definitely degraded by intermittent short circuits between accelerometer signal leak and the power return lead, the presence of which was verified during post-test inspection.

Figure 4-4 compares the impact shock data, from which can be seen a definite similarity in shape.

4.1.4 DISCUSSION AND ANALYSIS

a. Test #1 (S/N #2). An integration of the deceleration experience by the S/N #2 sphere during its 426 ft/sec impact reveals that the limiter absorbed a velocity increment of approximately 260 ft/sec prior to bottoming. Thus upon completion of the limiter stroke there remained 166 ft/sec of residual kinetic energy which masked the interpretation of any normal failure modes which may have been present.

Based on the integral of the recorded deceleration curve the velocity at which survival would have been expected is 392 ft/sec, viz.,

$$V = [\ (426)^2 - (166)^2\ ]^{1/2}$$

Based on Philco-Ford's simplified analytical model (which assumes no payload breakaway and which neglects stop mass effects and shock wave energy dissipation) the predicted survival velocity would be 378 ft/sec, viz.,

FIGURE - 4-1
IMPACT LIMITER S/N 2 TEST DATA

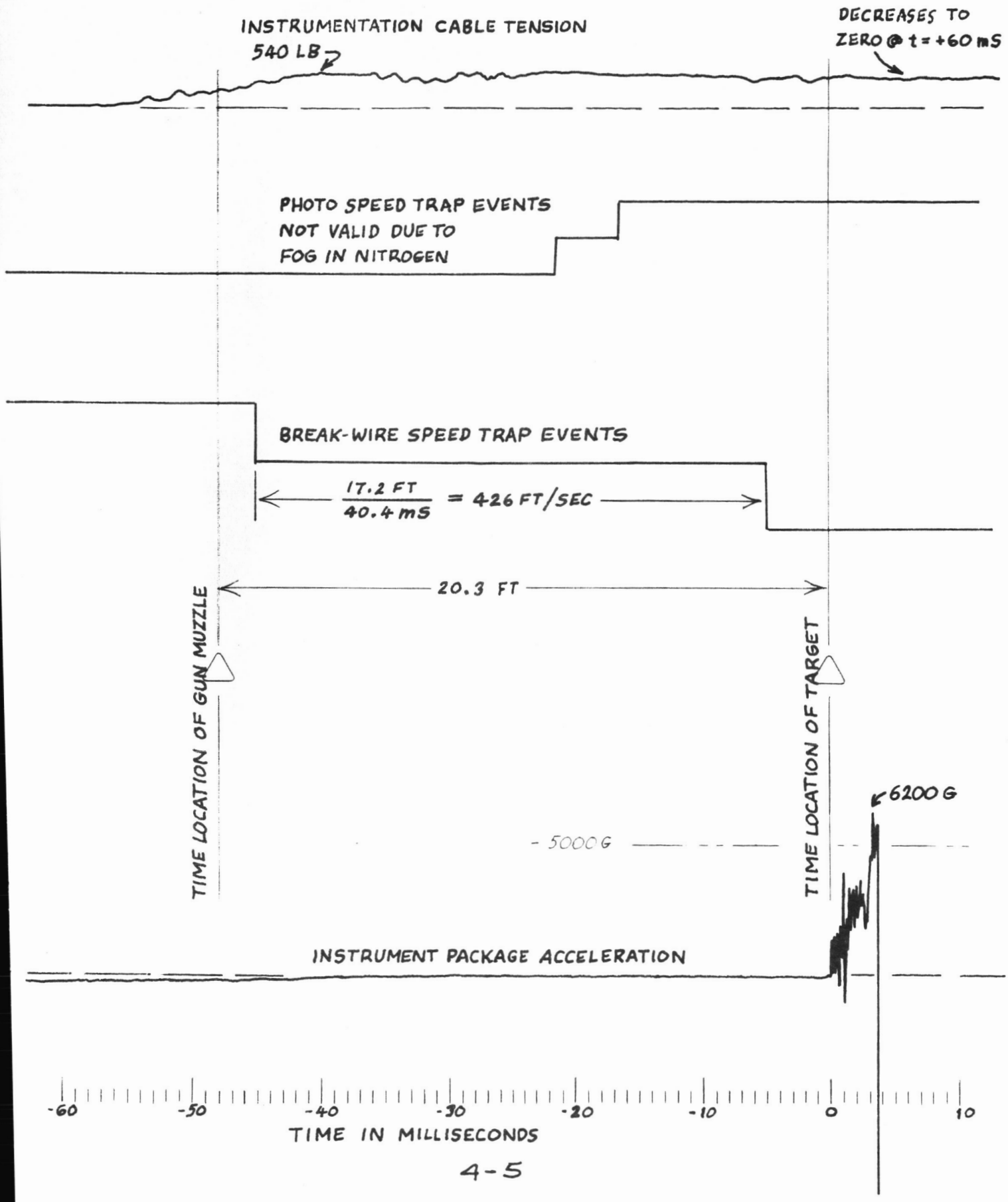

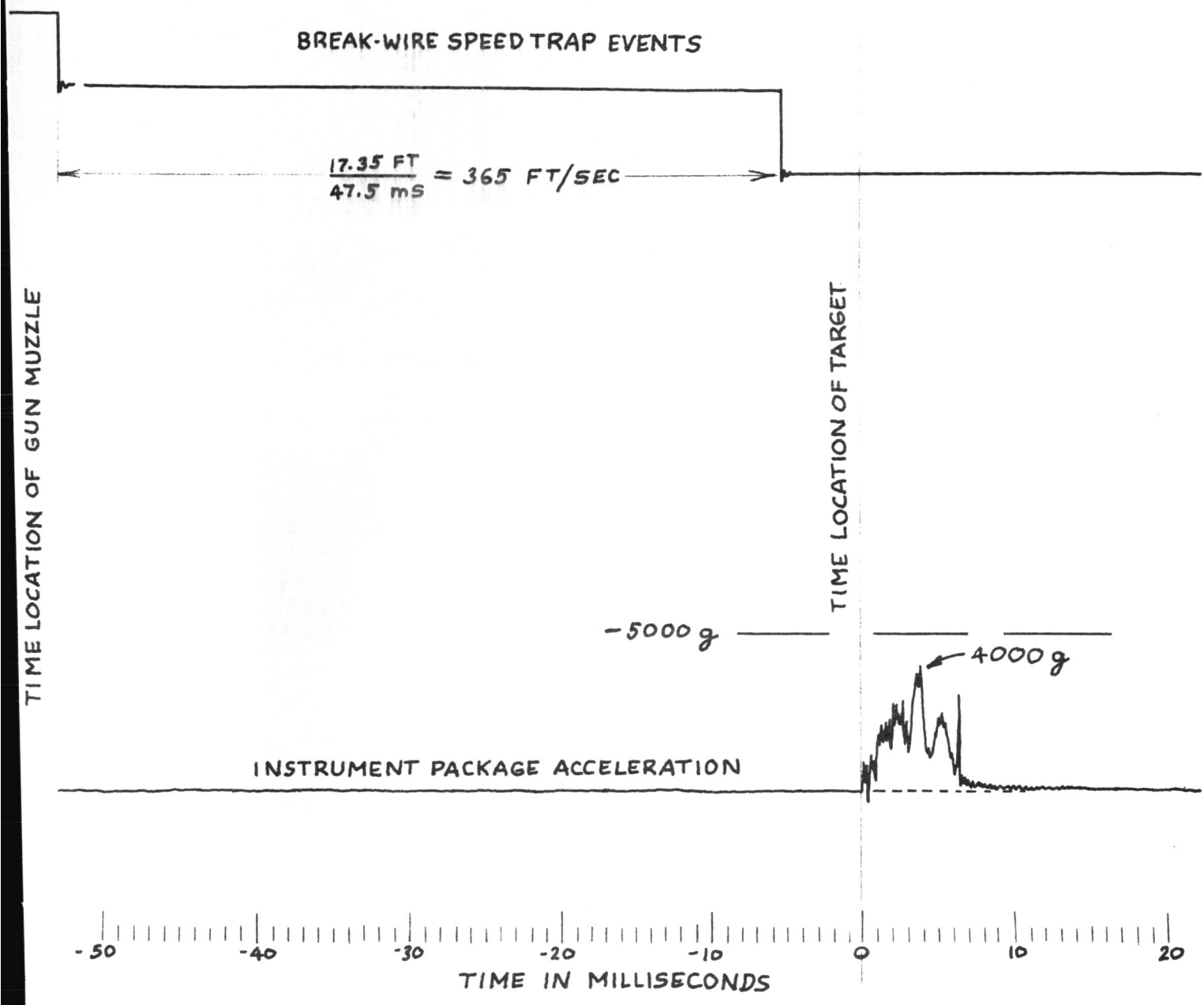

FIGURE 4-2
IMPACT LIMITER S/N 3 TEST DATA

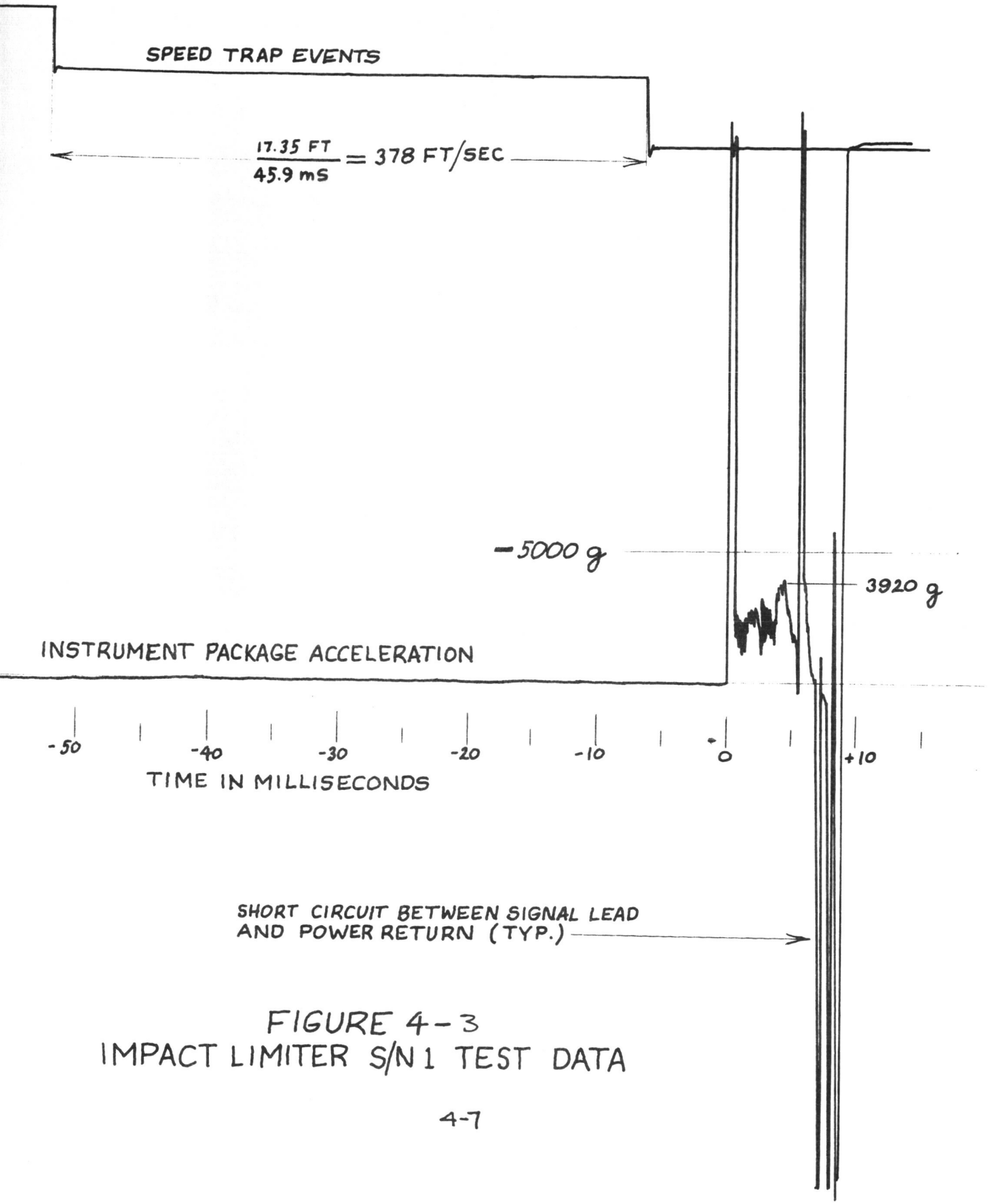

FIGURE 4-3
IMPACT LIMITER S/N 1 TEST DATA

FIGURE 4-4

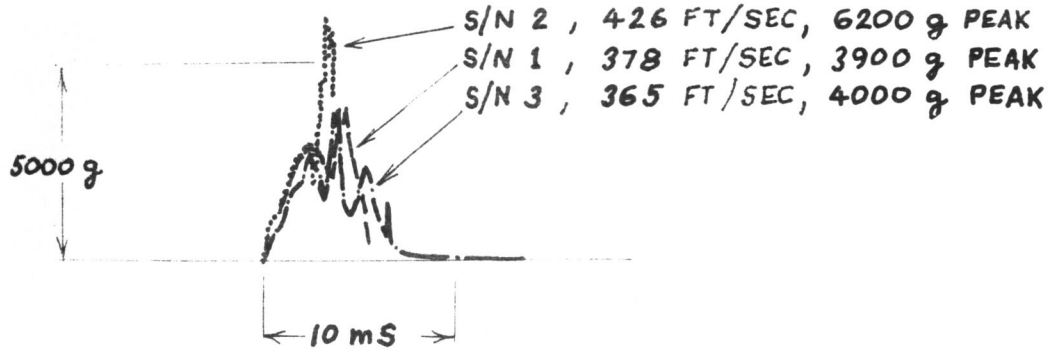

COMPARISON OF IMPACT WAVEFORMS

$$V^2 = \frac{\sigma_o\, g \left\{ (1-\alpha)\left[1 - Y_o^3 \left(1 - 3 \ln Y_o + 3/2\, \alpha\, (2 - 3 Y_o + Y_o^3)\right)\right]\right\}}{3\, \rho_1 \left[1 - Y_o^3 \left(1 - \frac{\rho_p}{\rho_1}\right)\right]}$$

Where

σ_o = 1500 psi

ρ_1 = balsa density = 9 lb/ft^3

ρ_p = "payload density"= 88 lb/ft^3 (conservative; assuming 50 pcf increases velocity capability 5 percent)

$$Y_p = \frac{r_p}{R} = \frac{7.5}{22.5} = .334$$

$$Y_o = \frac{r_o}{R} = Y_p\,(1 - \varepsilon) + \varepsilon = .334\ (.8) + .2 = .467$$

$$\alpha = \frac{\alpha_c}{\sigma_o} = .10$$

Substituting,

$$V^2 = \frac{(1500 + 144)(32.2)\{(1.9)[1 - (.101)(3.26) + .15\ (2.0 - 1.4 + .10)]\}}{(3)\ (9)\ [1 - (.037)(-8.8)]}$$

V = 378 ft/sec

It is apparent that based on the deceleration data (and the analytical model) that the 426 ft/sec impact condition for the first test sphere exceeded the limiter velocity capabilities by 9 percent. This corresponds to an excess energy condition of 18 percent. For this reason any evaluation of test results in terms of contributory failure mechanisms is not valid since it is not evident which failures were part of the "normal failure model" and which were attributable to excessive impact velocity.

b. Test #2 (S/N #3) and Test #3 (S/N #1). The next two tests were conducted at velocities consistent with the predictions of Test #1 and the analytical model (Table 4-1). Construction of the spheres was identical with the exception that the S/N #3 limiter contained 2 percent moisture while the S/N #1 limiter contained 8 percent moisture. From all physical evidence the failure experienced by both spheres upon impact was quite

similar in nature (Figures 4-1 thru 4-4). A normal 80 percent stroke footprint was incurred; peak decelerations were limited to an acceptable 4000 g's, however, in both cases a catastrophic splitting of the limiter occurred sometime during the deceleration stroke which resulted in the disgorgment of the payload and the breaking up of the limiter and its associated cover to numerous pieces. It was apparent that an immediate cause of this failure was (1) splitting of the exterior fiberglass cover, and (2) the presence of an inferior bond between the payload and the balsa. Since these are factors to which design improvements may be applied (as opposted to the balsa wood whose inherent structure is fixed) it is expeditious to consider the elements which contributed to their failure.

(1) Exterior Cover Failure. The exterior fiberglass cover split catastrophically during impact. It is suggested that this occurred as a result of payload breakaway (cannon-balling) during the deceleration stroke. It is surmised that this breakaway (and consequent cover splitting) occurred prior to the 4000 g peak in the deceleration stroke, since loads of this peak magnitude would have resulted in local cross-grain crushing of the balsa wood in the equatorial region of the limiter and there was no crushing of this nature in evidence.

(2) Payload Breakaway. The evidence supporting payload breakaway is substantial. Figure 4-5 presents the impact limiter geometry. A photograph of what appears to be segment a-b-c (based on geometry at point a) from the S/N #3 test sphere is shown in the background of Photo 66-3933. A similar piece for the S/N #1 test sphere is shown in Photo 66-4051. (Photographs are in the attachments of Section 4.1.5). It is revealed that there is complete crushing on the inside of the limiter (adjacent to the payload) but none on the outside (which is presumably within the crushed footprint). In addition, a measurement of the segment confirms that the length of the uncrushed portion (8 in.) corresponds exactly with the distance a-b of Figure 4-5. Thus a priori physical evidence is presented that the payload "cannonballed" forward in the limiter (and split the cover) prior to the time the footprint extended past point 'a' of Figure 4-5.

Let us consider next the theoretical payload deceleration loads to initiate payload breakaway. Referring again to Figure 4-5 it may be seen that the vertical component of the parallel grain contribution to the resisting force on the payload element d φ is

$$d F_{V_o} = 2\pi \sigma_o R_p^2 \sin \varphi \cos \varphi \, d \varphi$$

Integrating between limits $\varphi = 0$ and $\varphi = \varphi_b$ and setting equal to the peak inertial loads imposed by the payload during impact we obtain an expression for φ_b which when solved defines the required minimum bearing area at the base of the payload to avoid breakaway; thus,

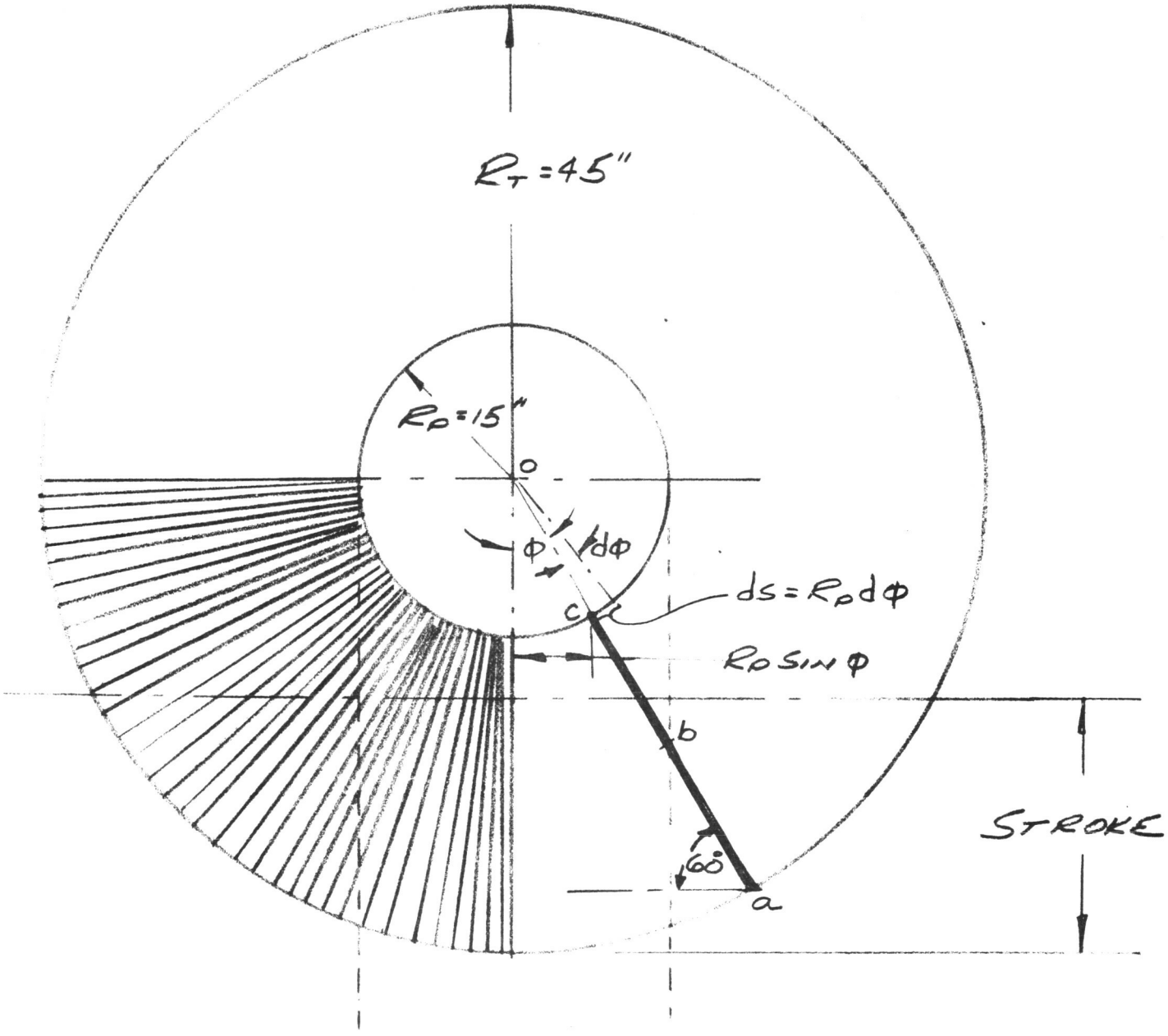

IMPACT LIMITER GEOMETRY

Figure 4-5

$$F_V = 2\pi R_p^2 T_o \int_o^{\varphi_b} \sin\varphi \cos\varphi \, d\varphi$$

or

$$\sin^2 \varphi_b = \frac{F_V}{\pi R_p^2 \sigma_o}$$

substituting

$$\sin^2 \varphi_b = \frac{(50 \text{ lb}) \quad (4000)}{(\pi)(7.5)^2 \quad (1500)}$$

solving

$$\varphi_b \simeq 60^o$$

Examination of Photos 66-3981 and 66-4048 (see Section 4.1.5) reveals that for the two test payloads in question bonding may well have been absent in the 30 degree region extending below the equator. Thus, it can be stated that conditions sufficient to warrant payloads breakaway were present.

(3) Consequences of Payload Breakaway. At loads sufficient to cause payload breakaway (and internal crushing of the balsa wood) a hoop stress is induced in the lower portion of the limiter which is sufficient to cause rupture.

Assume that the maximum normal strees which can be imposed on the cover is equal to the compression crush strength of the balsa. If we then ignore any support in shear from adjacent elements (which appears justified based on the multiple radial shearplane failures found in the limiter following impact) we obtain the following circumferential load distribution in the cover:

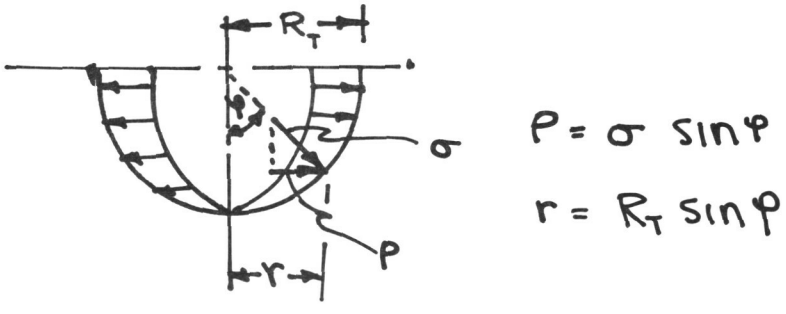

Since it has been established that the payload breaks away, then the hoop tension loads may be assumed to be as described by this function. Hence, the hoop stress in the cover as a function of φ is

$$\sigma_T = \frac{\sigma_o R_T \sin^2 \varphi}{t}$$

Assuming an ultimate tensile strength for fiberglass of 30,000 psi and solving for φ we obtain the angle above which rupture will occur.

$$\sin^2 \varphi = \frac{\sigma_T t}{\sigma_o R_T} = \frac{(30,000)(.04)}{(1500)\quad(22.5)} = .0356 \qquad \text{or } \varphi = 11^o$$

Thus, even neglecting the severe bending stresses and accompanying tears which occur in the cover at the edge of the footpring due to the sharp bend radius formed we have established that sufficient conditions exist to initiate rupture of the cover. Once a tearing has been intiaited there is very little to stop its propagaion, since the material possess inherently low tear resistance.

d. Bond Failure. Propagation of the cover initiated failure is aggravated by the presence of a poor bond between the payload and the limiter. In the absence of this bond any loss of cover continuity results in the complete disintegration of the limiter as was experienced in the subject tests. While it is felt that the quality of this bond is not critical to payload survival it is thought the bond plays an important part in maintaining limiter integrity.

The payload and limiter surfaces were fit checked and thoroughly cleaned with compressed air and MEK prior to assembly. Assembly was performed in a vacuum bag under one atmosphere of pressure using what was considered to be an excess of resin. The inferior quality bond which resulted can only be explained in retrospect as being the result of a combination of the following contributory factors:

(1) Distortion of the inner hemisphere and equatorial surfaces of the limiter due to de-moisturization. This resulted in a poorer than average fit for the assembly and increased the excess resin requirement. The importance of this factor is evidenced by the S/N #1 limiter which was assembled without de-moisturization; it showed no excess resin in the bond line following test.

(2) The presence of dynamic "peel" loads at the resin interface during impact.

(3) Inadequate roughening or surface treatment of the maple payload to achieve the required adherence.

(4) Entrapment of air in the bond line during mating of the spherical parts. This could result in either a dry spot within the bond line or a driving out of the required excess resin during vacuum bagging.

(5) The inability of one atmosphere of pressure to drive excess resin from the system through a 15 in. long bond line during the final assembly vacuum bag process.

4.1.5 POST TEST SPHERE EXAMINATION

Photographs were taken of the impact balsa segments after each test. The pieces were gathered, reassembled, and arranged so that the failures modes would be recorded. This allows comparison from test to test and provides visual information to those who had not witnessed the test. Some postulations of improvements may come long after the present program. The impacted sphere photographs are presented in the following order:

a. Test #1 (S/N #2)

Photo 66-3886	Balsa Shell Fragments
Photo 66-3887	Payload Impacted Surface

b. Test #2 (S/N #3.

Photo 66-3981	Payload Top View
Photo 66-3982	Payload Impacted Surface
Photo 66-3983	Balsa Shell Fragment
Photo 66-3932	Arranged Crushed Balsa Segments
Photo 66-3933	Balsa Segments with Internal Crushing
Photo 66-3934	Upper Hemisphere Reassembled Top View
Photo 66-3935	Upper Hemisphere Reassembled Internal View
Photo 66-3936	Payload Cavity Uper Hemisphere
Photo 66-3937	Crushed Balsa
Photo 66-3938	Upper Hemisphere Reassembled Side View

c. Test #3 (S/N #1)

Photo 66-4089	Balsa Shell Fragments
Photo 66-4090	Payload Top View
Photo 66-4091	Payload Bottom View
Photo 66-4048	Payload Impacted Surface

60

Photo 66-4049	Arranged Crushed Balsa Segments
Photo 66-4050	Payload Cavity Upper Hemispheres
Photo 66-4051	Balsa Segment with Internal Crushing
Photo 66-4052	Payload Top Surface
Photo 66-4054	Upper Hemisphere Reassembled, Left
Photo 66-4056	Upper Hemisphere Reassembled, Right
Photo 66-4057	Upper Hemisphere Reassembled, Bottom

Photo 66-3886 Balsa Shell Fragments

Photo 66-3887 Payload Impacted Surface

Photo 66-3981 Payload Top View

Photo 66-3982 Payload Impacted Surface

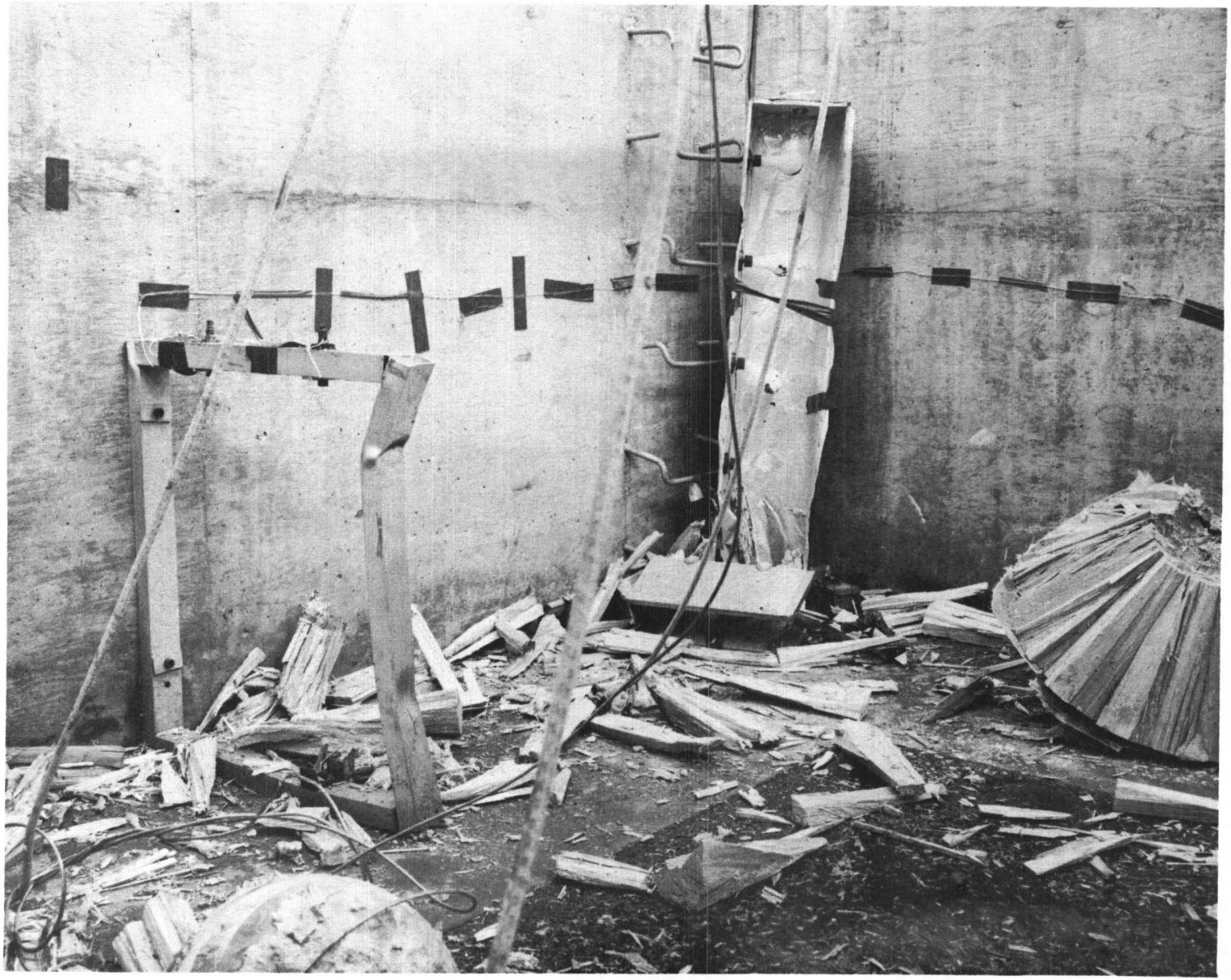

Photo 66-3983 Balsa Shell Fragment

Photo 66-3932 Arranged Crushed Balsa Segments

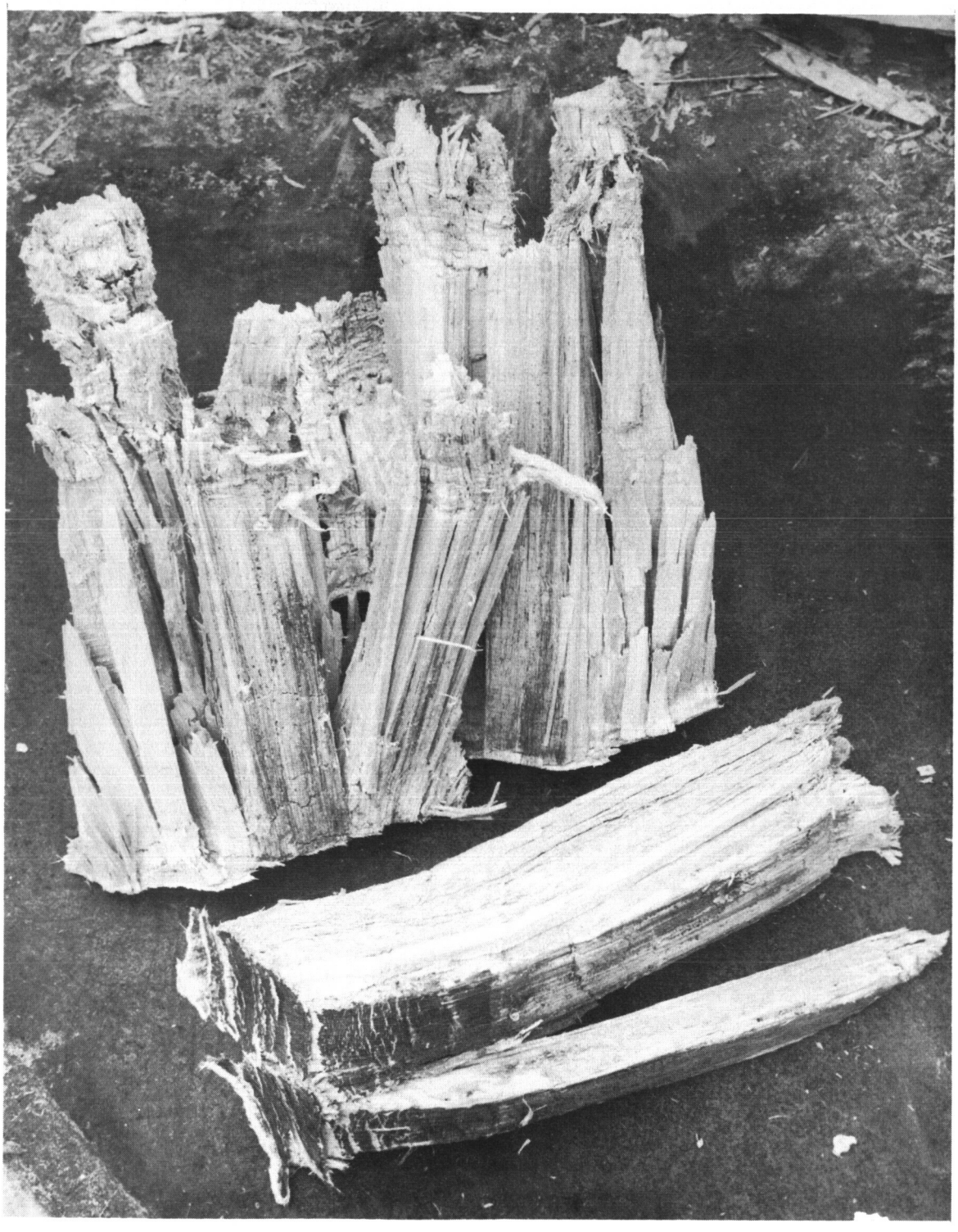

Photo 66-3933 Balsa Segments with Internal Crushing

Photo 66-3934 Upper Hemisphere Reassembled Top View

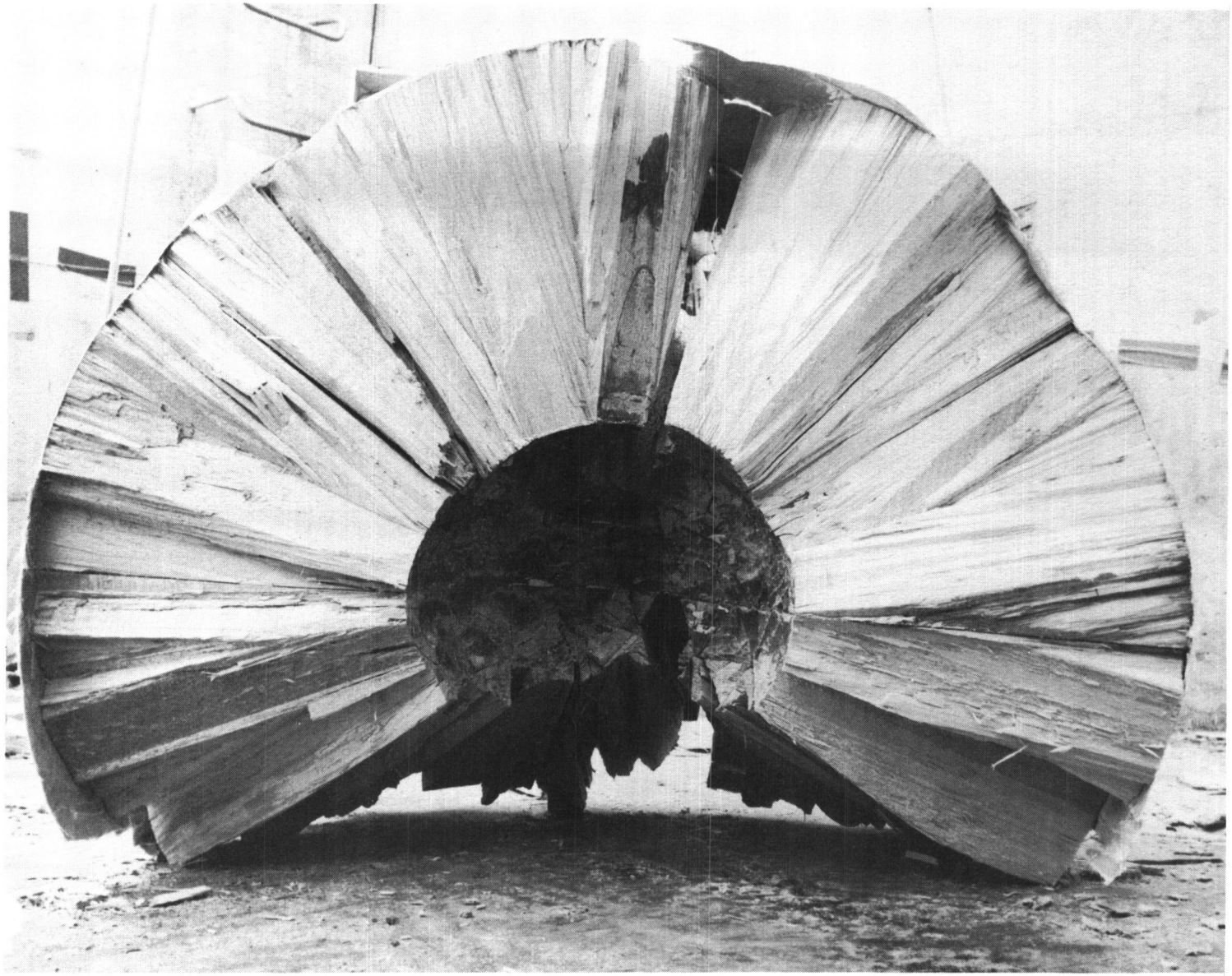

Photo 66-3935 Upper Hemisphere Reassembled Internal View

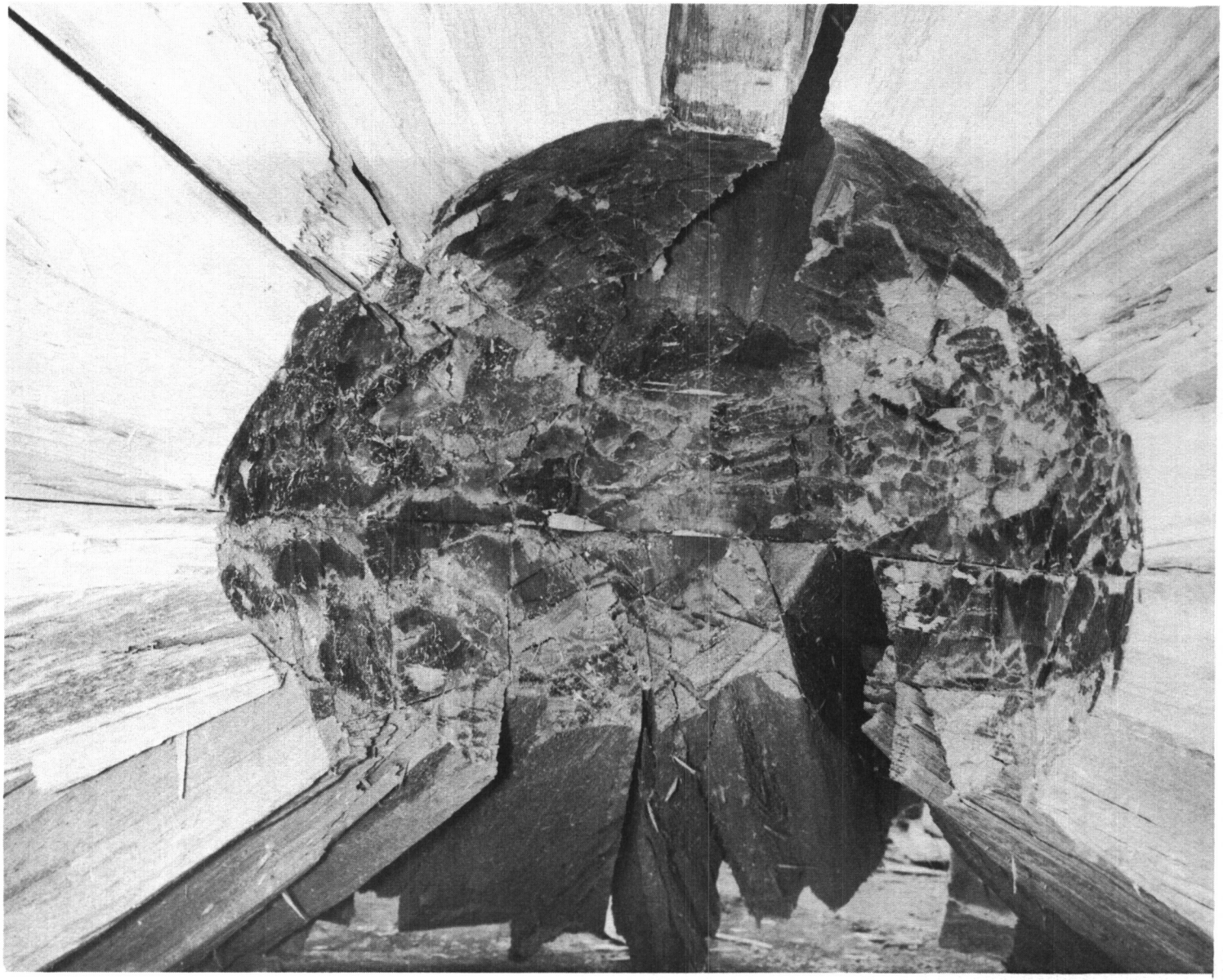

Photo 66-3936 Payload Cavity Upper Hemisphere

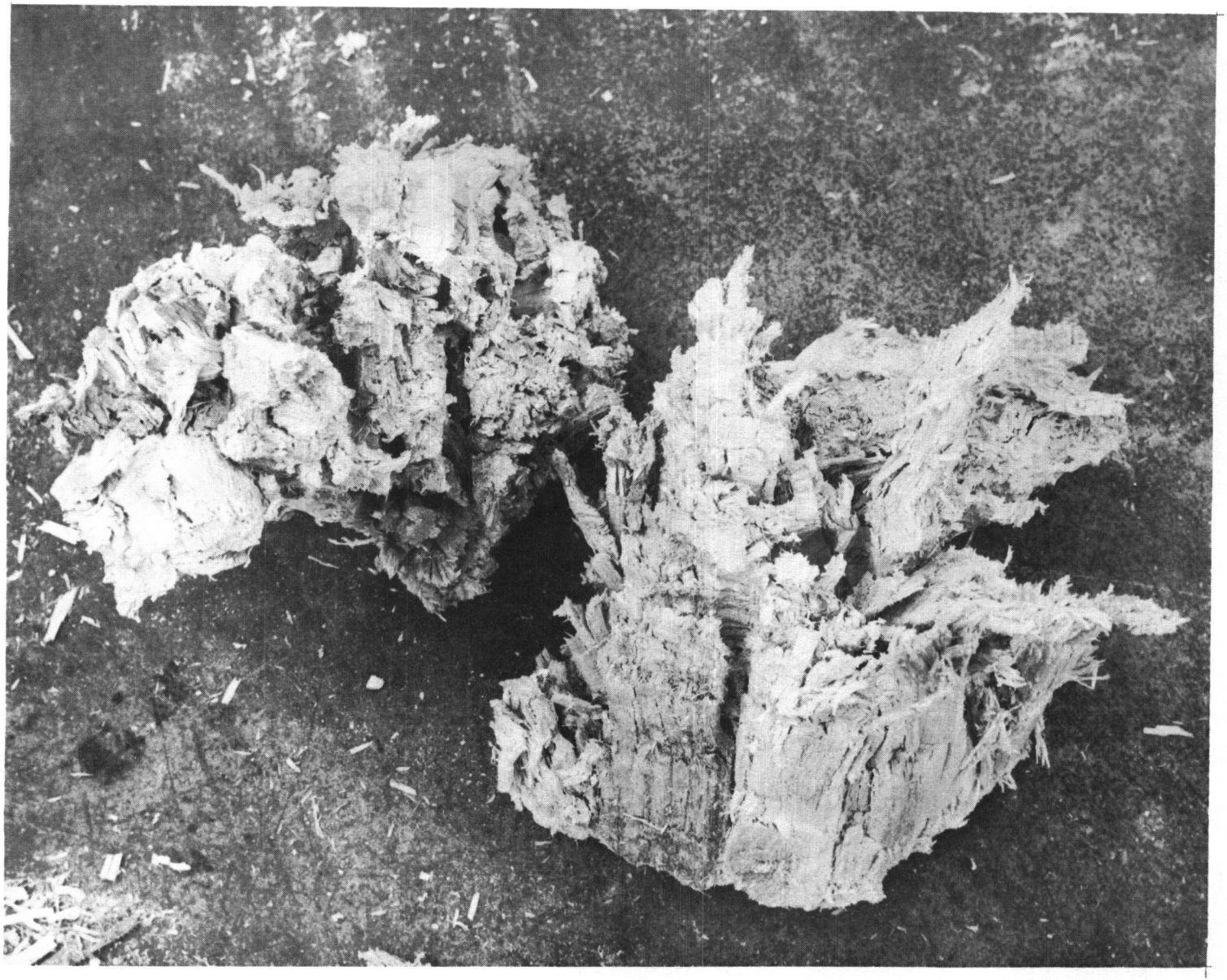

Photo 66-3937 Crushed Balsa

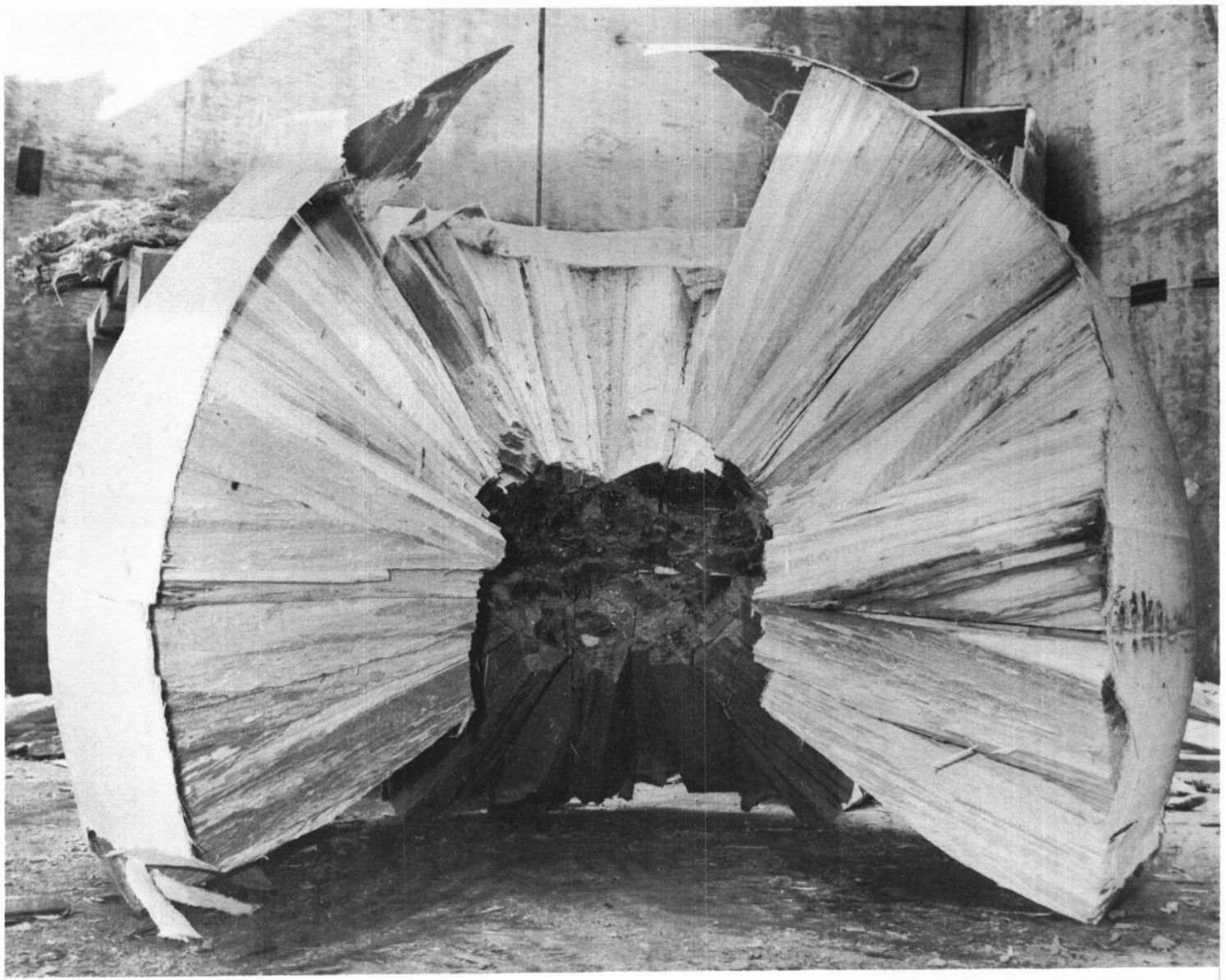

Photo 66-3938 Upper Hemisphere Reassembled Side View

Photo 66-3089 Balsa Shell Fragments

Photo 66-4090 Payload Top View

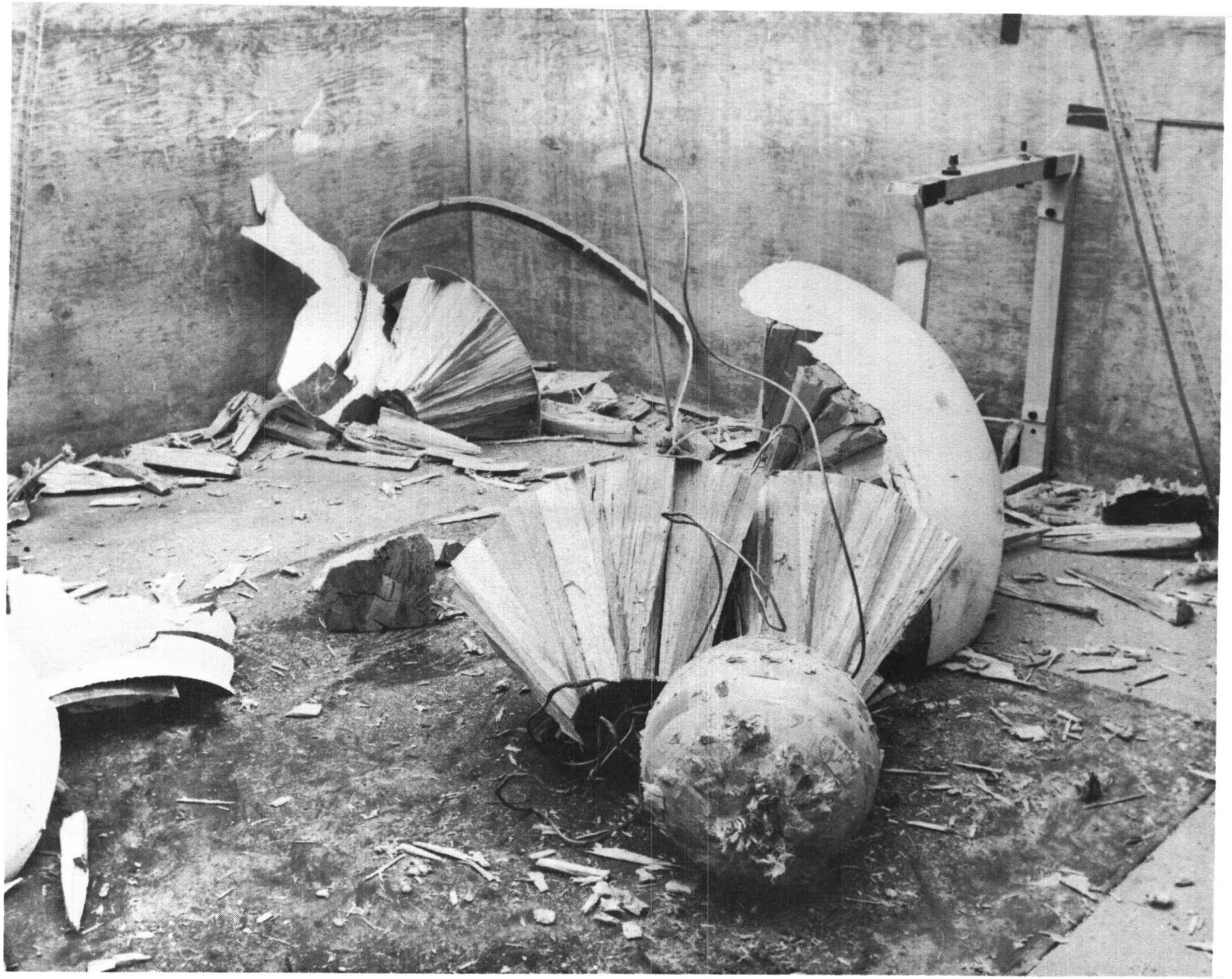

Photo 66-4091 Payload Bottom View

Photo 66-4048 Payload Impacted Surface

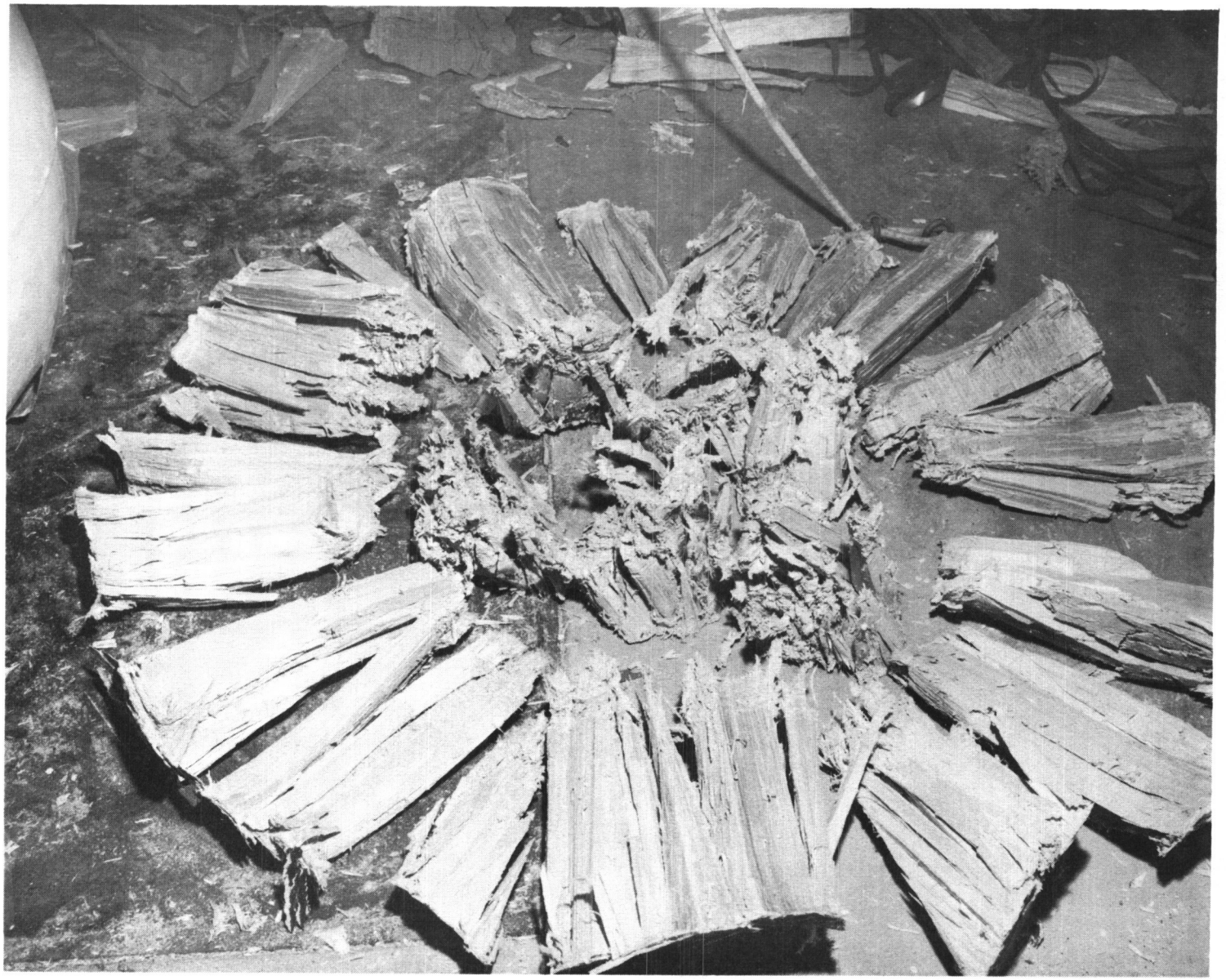

Photo 66-4049 Arranged Crushed Balsa Segments

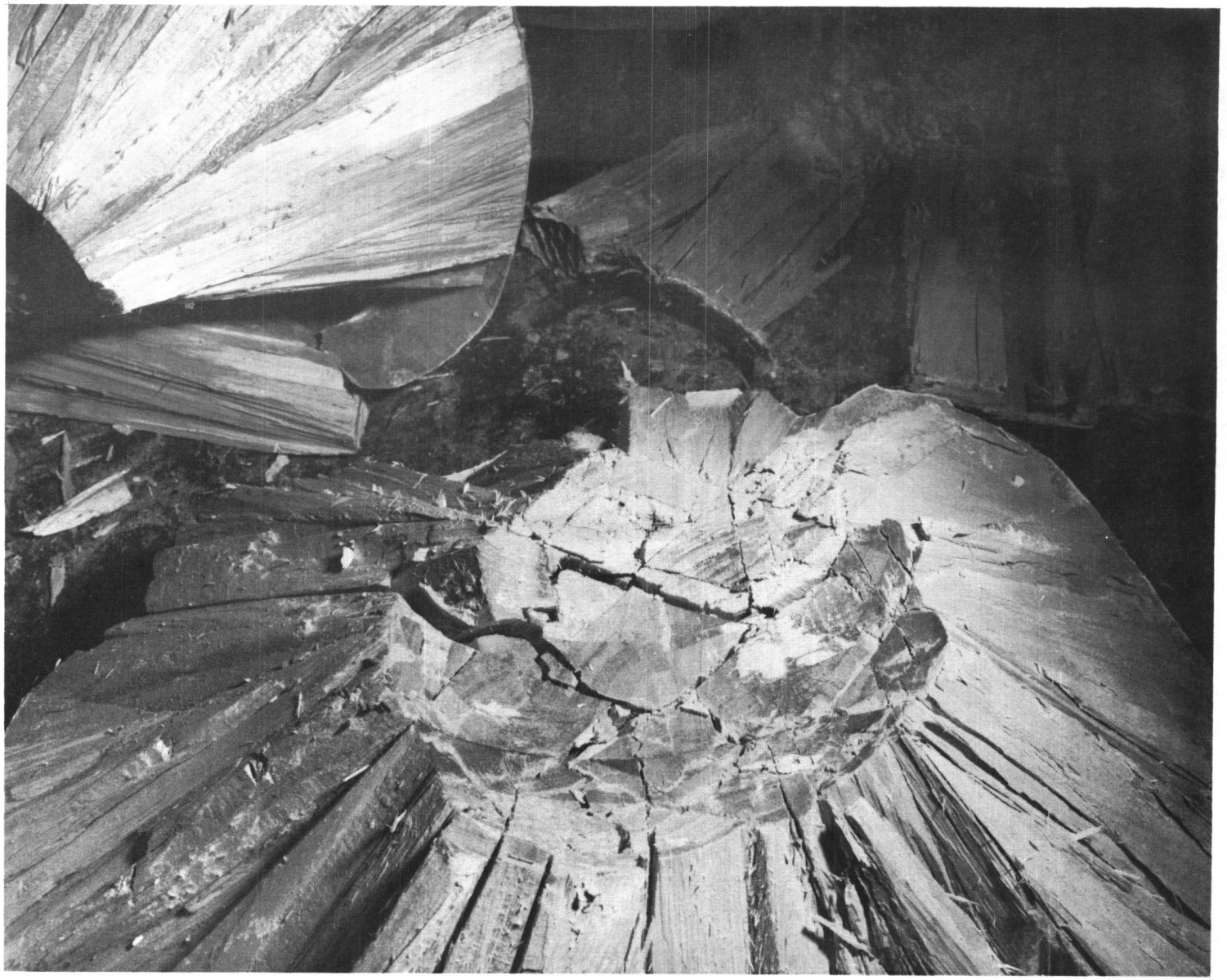

Photo 66-4050 Payload Cavity Upper Hemisphere

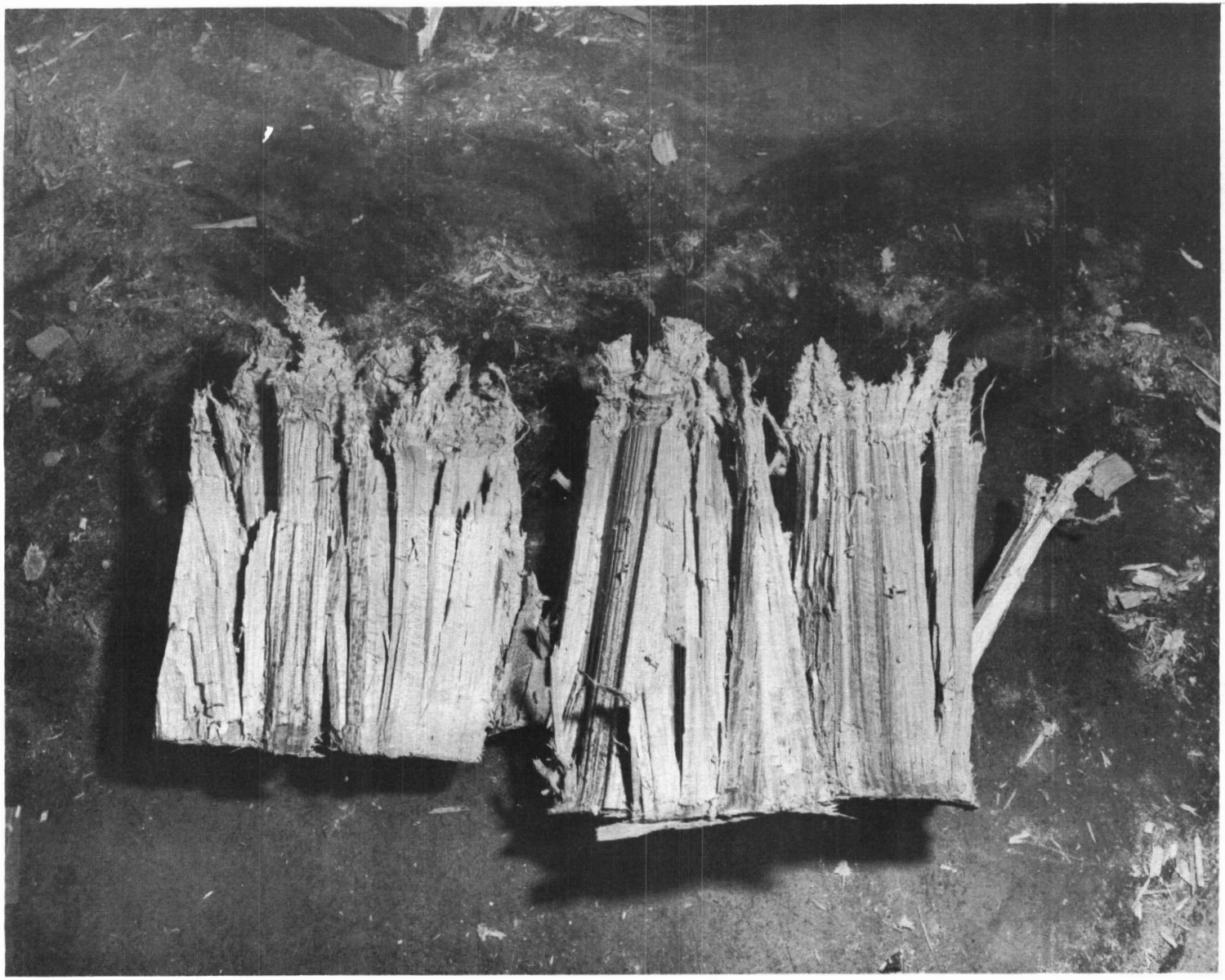

Photo 66-4051 Balsa Segment with Internal Crushing

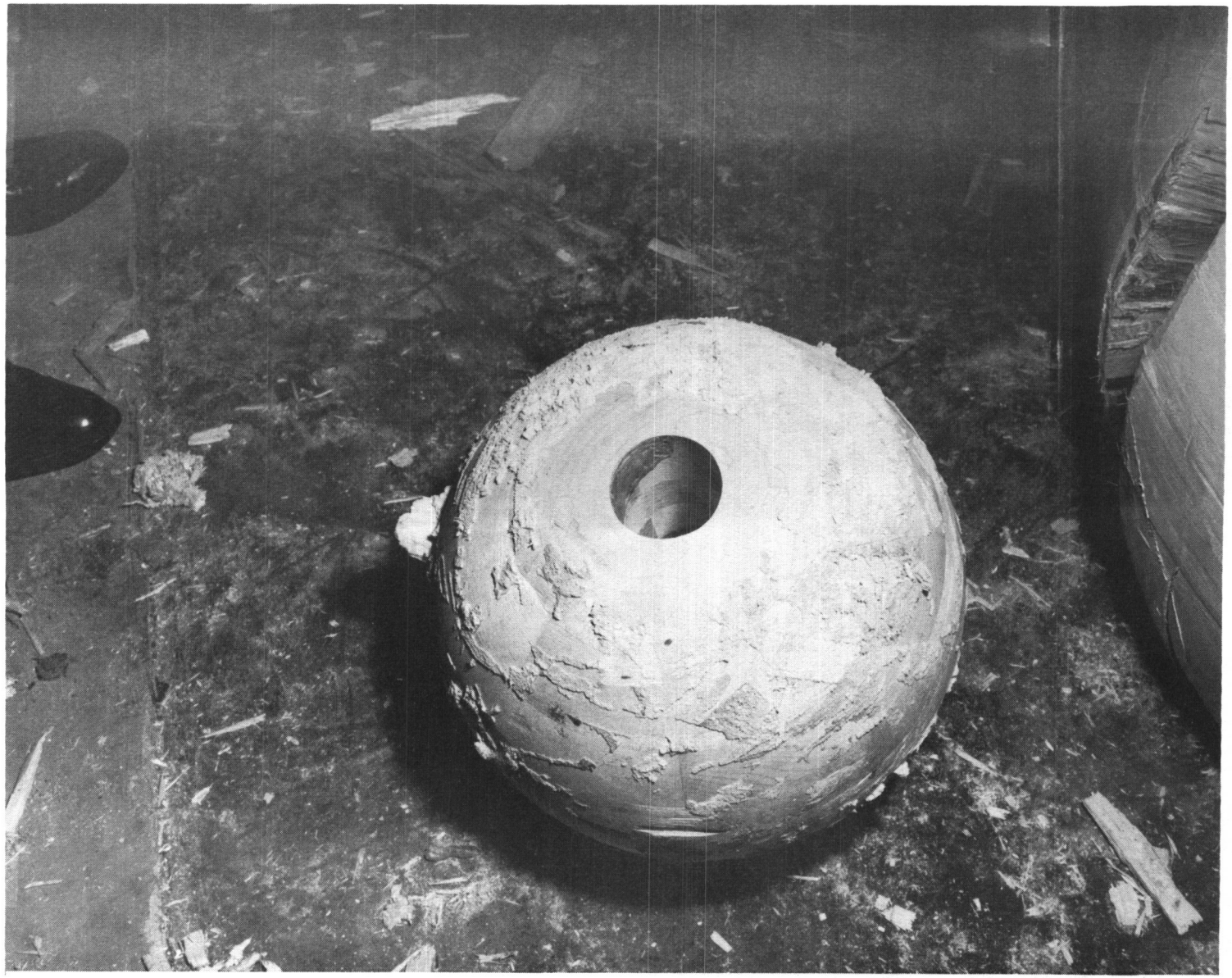

Photo 66-4052 Payload Top Surface

Photo 66-4054 Upper Hemisphere Reassembled, Left

Photo 66-4056 Upper Hemisphere Reassembled, Right

Photo 66-4057 Upper Hemisphere Reassembled, Bottom

4.2 TEST REPORT ON SERIAL NO. 4 BALSA SPHERE

4.2.1 TEST RESULTS

Impact Limiter S/N #4 with hardwood payload and shock instrumentation left the blowgun muzzle at 374 ft/sec and impacted against a reinforced concrete seismic block. The limiter structure stayed intact, limiting the shock deceleration of the internal instrument package to 4320 g. The specimen experienced a partially elastic rebound which was sufficient to carry it back up to the gun muzzle. The average rebound speed over the 10-ft interval just below the gun muzzle was computed from motion picture data as approximately 38 ft/sec. Table 4-II presents a summary of the important data.

TABLE 4-II

SUMMARY OF TEST DATA

Date of Test:	28 January 1967
Specimen:	Large Impact Limiter S/N #4
Gross Weight:	342 lbs
Peak Acceleration:	290 g
Peak Deceleration:	4320 g
Speed at Impact:	374 ft/sec
Impact Footprint:	43 in. diameter

High-speed motion coverage was provided at the blow-gun breech, ground level, and target level. No data were obtained from the breech camera due to the presence of a dense water cloud obtained from the adiabatic cooling of pressurized nitrogen gas below its dew point. The ground level camera data indicated that the projectile left the blowgun muzzle without any discernable tip-off or spin rate. The rebounding projectile was also recorded as having an average speed of 38 ft/sec over the 10-ft interval just before it struck the gun muzzle. The target-level camera recorded the impact event, but the dense water cloud obscurred the specimen from camera view before the impact had been completed. There were no failures recorded by any of the three camreas.

Figure 4-6 is a tracing of the oscillogram obtained during the test. The acceleration time-history is approximately triangular having a peak value of 4320 g and a duration of seven milliseconds. The short duration discontinuity which occurs at t = +9 milliseconds is attributed to a momentary cable fault. It does not obscure data since the impact had been completed by that time

4.2.2 SPECIMEN DESCRIPTION

The design improvements discussed in Section 3.9 of this report were introduced into the fabrication of the subject S/N #4 test sphere.

The final sphere assembly was performed using the Epon 828/Versamid 140 resin system in a 1 to 1 ratio by weight. This resin system was selected for its demonstrated capability to resist dynamic peel loads in excess of the strength of the internal maple payload (and the balsa wood). The internal payload was first fit checked using colored chalk to ascertain the location of any high spots; these were removed by sanding of the balsa. The payload was then highly abraded with sandpaper; the interior balsa wood and payload surfaces thoroughly cleaned with compressed air; and the payload treated with MEK. All mating surfaces were then sealed with a 20 percent non-volatile primer mixture of 828/140 resin and MEK. This was allowed to cure for 2 to 12 hrs.

Installation of the payload sphere was accomplished in two steps. First resin was puddled in the inverted upper balsa hemisphere. The payload was then slowly lowered into position and the excess resin allowed to flow out and be wiped away at the equator. The assembly (less upper hemisphere) was then loaded with a 500 lb weight and allowed to cure overnight. Prior to installation of the upper hemisphere four (approximately 1/8 in.) radial grooves were provided in the hemispheres' equatorial plane to provide a flow path for extraction of excess resin. The lower hemisphere was then installed in a manner identical to the upper hemisphere. An excellent fit was achieved; only two pounds of resin were required for the final assembly process. This represents an average glue line of less than 0.020.

The cover was installed on the assembled sphere in three steps. The exterior was first sealed with the dilute 828/140 resin system. Next the surface was coated with the Adiprene L-160 (100 pts)/MOCA (11 pts) Urethane adhesive system and the ballistic nylon cover segments placed into position and coated with additional resin as required. It was found that the heavy gauge material selected was extremely difficult to work; this required each cover layer to be applied in 13 pieces with 2-in. overlaps. The pattern consisted of 6 pie-shaped segments (top and bottom) and an 18-in. wide equatorial band. It is thought that the selection of a more loose weave drapable fabric could significantly reduce the piecing overlaps and consequently weight of each cover layer. The first cover layer together with the balsa

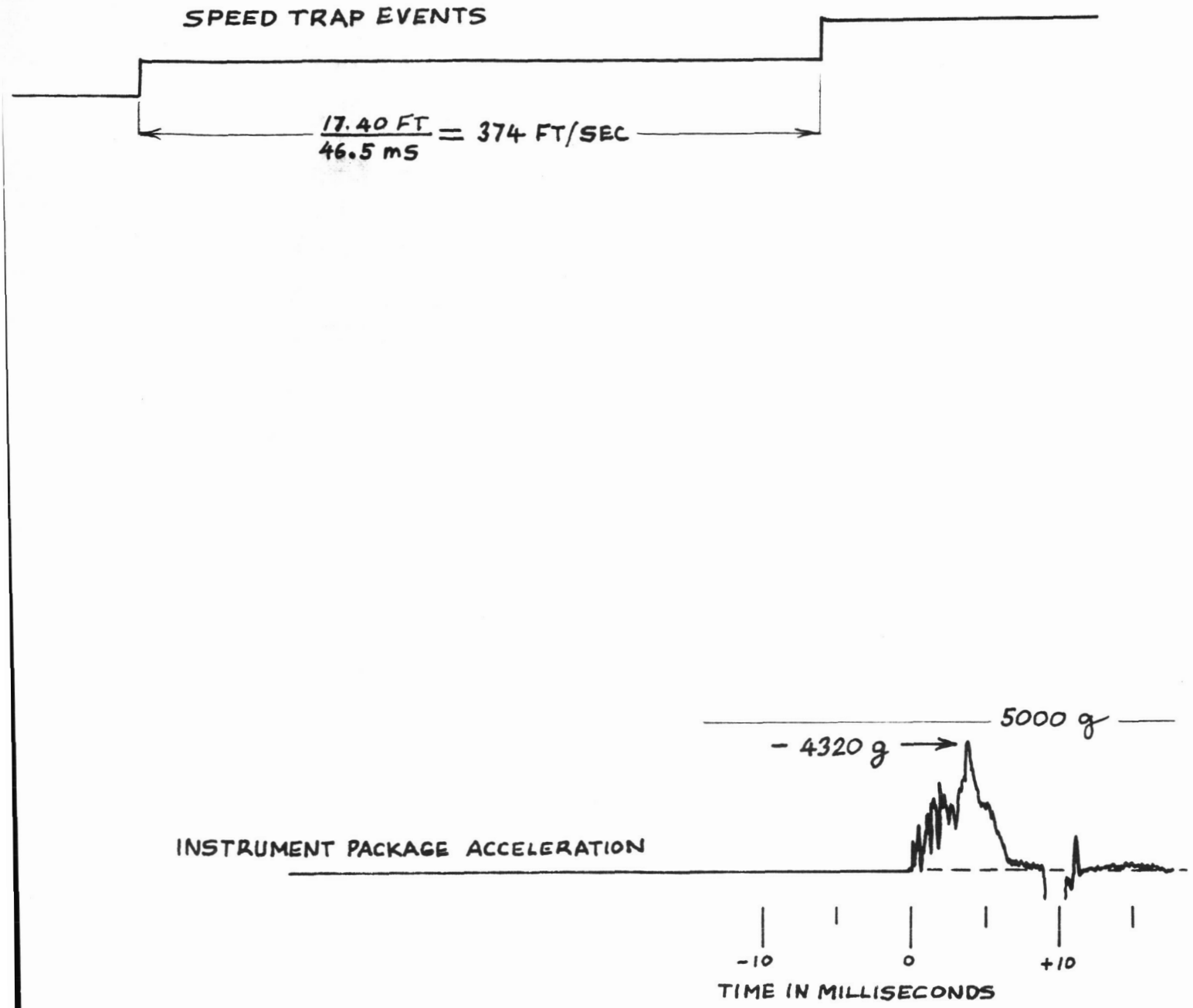

FIGURE 4-6
IMPACT LIMITER S-N 4 TEST DATA

primer weighed 19 lbs. The second and final cover layer which was applied in an identical manner weighed 10 lbs. This compares with approximately 23 lbs for the previous four-layer fiberglass cover system.

4.2.3 POST MOTRUM EXAMINATION

The condition of the test sphere following impact is documented in the photos in Figures 4-7, 4-8 and 4-9. The sphere had rebounded through the trap following impact and was found resting on the closed net as shown in Figure 4-7. A post motrum examination of the sphere revealed the following significant features:

(1) The limiter/payload assembly was in one piece.

(2) The payload had broken away from the limiter and "cannon-balled" forward in the balsa sometime prior to completion of the deceleration stroke. (Figure 4-8).

(3) The exterior cover was torn away in the vicinity of the footprint (Figure 4-9).

(4) Multiple vertical splits were present in the cover. (Figure 4-7). They extended from the periphery of the footprint to a point about 30° above the equator. The improved tear resistance of the redesigned cover appeared to have prevented a full 180° propogation of the tears and the accompanying complete disintegration of the limiter.

(5) There were radial segments of balsa at the periphery of the footprint which were crushed on the outside, and the inside, but not at the center (evidence of cannon-balling) (Figure 4-8).

(6) The balsa segments within the footprint had a physical appearance similar to that of pieces from previous tests. It appeared that a large portion of the wood at the periphery of the footprint incurred lateral crushing only (the wood fibers tending to bend outward rather than incur any axial crush).

(7) The bond of the payload to the balsa was excellent.

(8) The bond of the cover to the balsa was excellent.

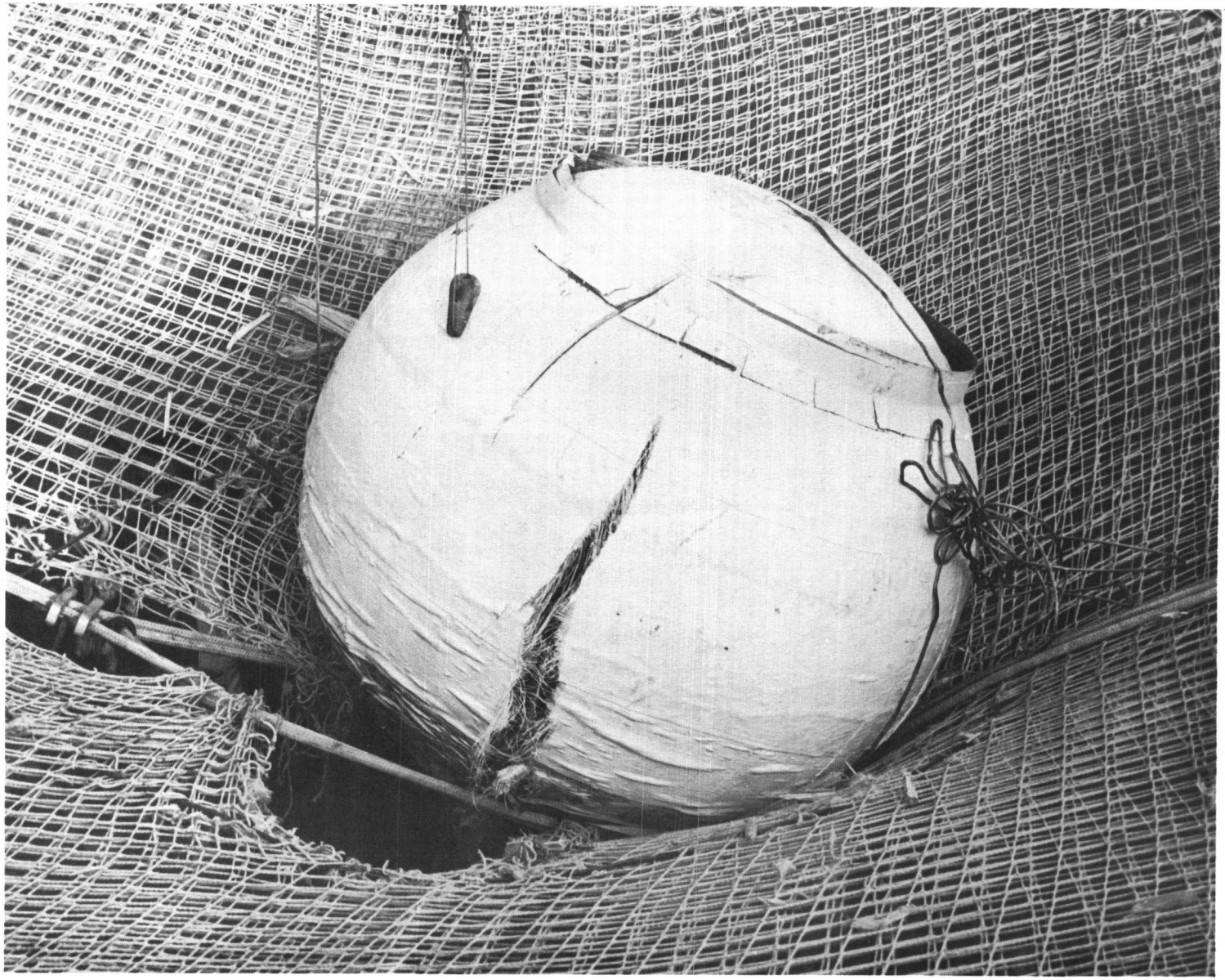

FIGURE 4-7 LIMITER S/N #4 AFTER TEST

FIGURE 4-8 FOOTPRINT INTERNAL VIEW, S/N #4

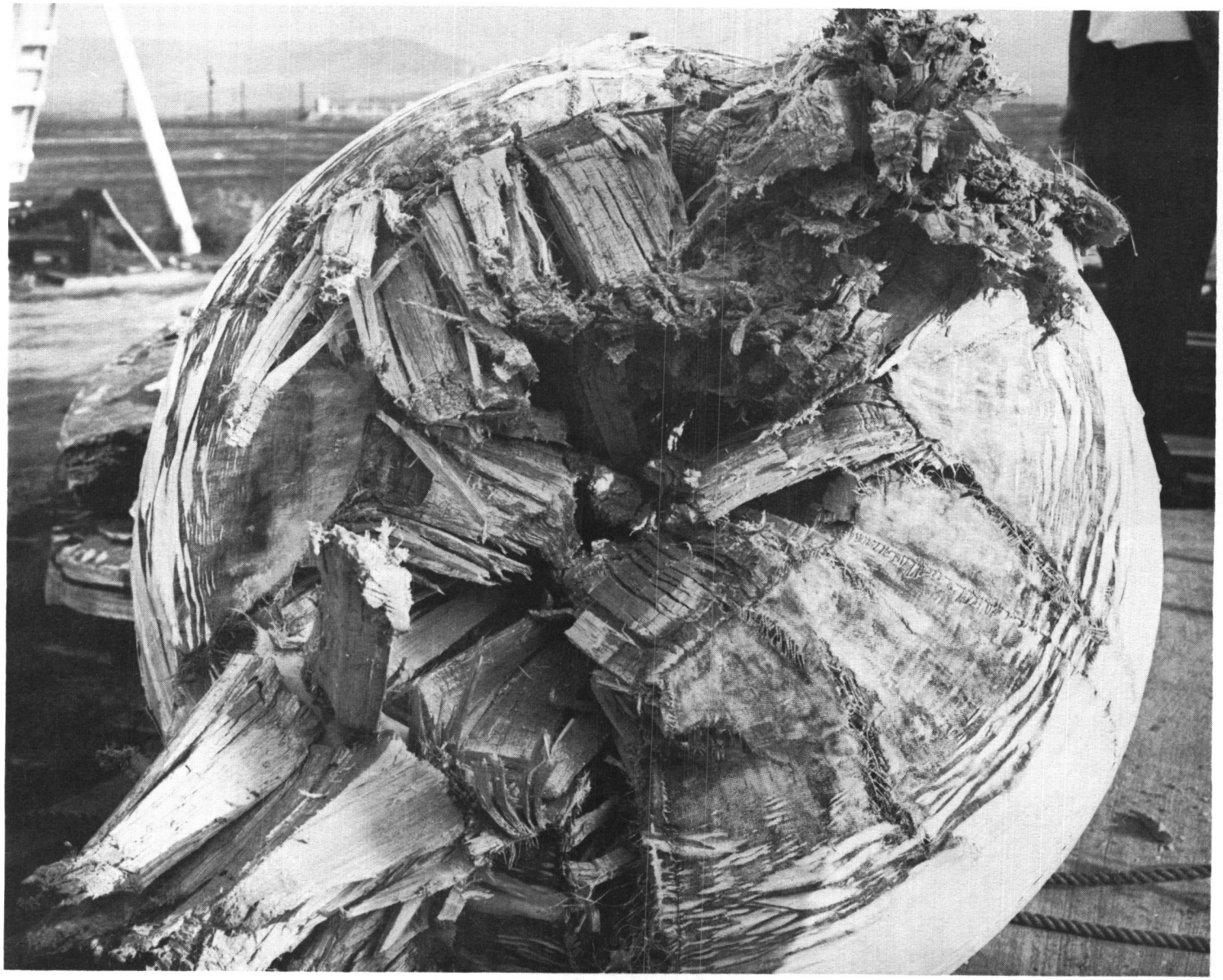

FIGURE 4-9 FOOTPRINT EXTERNAL VIEW, S/N #4

4.3 WEIGHT SUMMARY

Table 4-III summarizes the weight elements of the test spheres S/N #1 to S/N #4.

TABLE 4-III

WEIGHT SUMMARY -- BALSA WOOD IMPACT LIMITER
(15" I.D.; 45" O.D.)

	S/N #1	S/N #2	S/N #3	S/N #4
BALSA HEMISPHERES				
Upper	126.5 (9.5 pcf)	121.2* (9.1 pcf)	114.8* (8.6 pcf)	123.0 (9.2 pcf)
Lower	130.5 (9.8 pcf)	120.7* (9.1 pcf)	115.7* (8.7 pcf)	120.5 (9.1 pcf)
TOTAL	257.0	241.9	230.5	243.5
PAYLOAD				
Inner Payload	52.5	50.2	51.5	53.0
Payload Instrumentation	1.3	1.3	1.3	1.3
Final Assembly Resin	4.1	4.6	8.1	2.0
External Cover	20.0(1)	19.4(1)	24.9(1)	29.0(2)
Equatorial Girth Band	3.0(1)	3.0(1)	3.0(1)	--
External Fittings	6.6	9.6	5.2	6.7
TOTAL	87.5	88.1	94.0	92.0
TOTAL SPHERE WEIGHT(lbs)	344.5	330.0	324.5	335.5
AVERAGE MOISTURE CONTENT	8%	2%	2%	8%

* Post-demoisturization weight.

(1) Four (4) layers 181 fiberglass; Epon 828 (50 pts)/Epocast 985 (50 pts) Resin System.

(2) Two (2) layers JP Stevens 34163, Ballistic Nylon; Adiprene L-100 (100 pts) (MOCA(11 pts) Reson System.